2020

OPTOGENETIC GUIDE RNA PRODUCTION FOR SPATIOTEMPORAL REGULATION OF CRISPR/CAS SYSTEMS

Diego Augusto Velasquez Pulgarin

OPTOGENETIC GUIDE RNA PRODUCTION FOR SPATIOTEMPORAL REGULATION OF CRISPR/CAS SYSTEMS

by

Diego Augusto Velasquez Pulgarin

A Dissertation

Submitted in Partial Fulfillment of the

Requirements for the Degree of

Doctor of Philosophy

Major: Biomedical Engineering

The University of Memphis

December 2020

DEDICATION

To my parents. My Father, who instilled in me a love for science and knowledge, has never stopped encouraging my roving curiosity. My Mother, who taught me that only through perseverance and strength of will are worthy accomplishments attained, has never stopped encouraging me to persist when I falter.

ACKNOWLEDGEMENTS

I would like to acknowledge the enormous debt of gratitude I owe my advisors **Gary Bowlin** and **Alexander Espinosa**. Bowlin believed in me and this project when all I had was an idea and a PowerPoint deck. What followed was a tour de force of patience, mentorship, and encouragement. The most eloquent writer would also fail to express what his support has meant to me and my career. Alex has been the molecular biology guru that allowed this project to come to fruition. All that I know of genome engineering has been a direct result of working with him. Besides my father teaching me how to read, I cannot envisage a more influential figure in my scientific formation.

I would also like to mention two very influential people that have helped shaped my graduate career: **Eugene Eckstein** and **Marie Wahren-Herlenius**. Eckstein guided me through stormy waters with the foresight and calmness of a master captain. He also has a remarkable ability to integrate information and talking to him was always an absolute pleasure and journey in itself. Marie is the Oracle of Stockholm. I am extremely grateful to be able to form a part of her extended group, and her suggestions and guidance have been instrumental for me.

To my Swedish lab mates: **William Nyberg** thank you for teaching me so much about molecular biology. I have seldom learned so much in such a short period of time. May we meet each other again, preferably over a tall, cold beer. **Tilen Tršelič**, the proverbial gentleman and scholar, thank you for your contributions to this work. More importantly, thank you for your unconditional friendship, guiding me around gorgeous Slovenia, and for becoming the quintessential fishing buddy. Soon we'll change that to fly-fishing buddy… **Andrea Scheffschick** and **Sina Fuchs**, the German contingent, life at the lab would not be as pleasant without both of you. **Vijole Ottosson**, thank you for all your hard work to manage a smooth-

running lab, fun conversations, oh and for stocking the office candy jar, my sweet-tooth really appreciates it. To the rest of the greater MWH group, thank you for your camaraderie. To others that circumstance or time and distance have taken from me: **Eliane**, **Michael**, **Rita**, and **Nikos**; unforgettable, I hope our paths cross again.

To my UofM lab mates: **Hunter King**, thanks for your friendship and for keeping me updated on Memphis affairs. Good luck, but remember, stay away from the temptation of the triple crown. **Allison Fetz**, thanks for being a great role model, even though you are younger than I am. May I grow up to be similar. **William Cain**, Captain America, you are a true friend. Thanks for always making the lab a fun place to be, and for introducing me to your wonderful parents, helping me in my all-consuming pursuit of *Canis latrans*. Also thank all three of you for giving long range marksmanship a try… Lab range days are a dear memory. **Kasyap**, you are awesome… please visit r/kasyapisawesome for more information. To the rest of the Bowlin lab: maintain your tendency towards greatness.

Greg McGraw, it has been a privilege to be your friend. Few people have been so kind and loyal.

Cheyenne Rhodes, though we drifted apart, you have been one of the most important people in my life. Your support and selfless sacrifices were instrumental in making me who I am today. I will never forget you.

To my brothers: **Alejo** and **Chiqui** Thanks for sharing this crazy adventure of growing up with me. I miss both of you.

Sanna Vatanen, tack för allt. Vad skulle jag göra utan dig? Vetenskapsmorgon med Diego skulle bli ganska tråkigt utan min enda lyssnare.

To my Parents: **Augusto** and **Beatriz**, it is possible to win the lottery without buying a ticket, Dad… thanks for making me the luckiest kid in the world. Gracias por ser el ejemplo más edificante que he conocido. El mundo es enorme y la distancia nos separa, pero siempre están en el fondo de mi corazón.

Finally, dear reader, if you find yourself alone, flipping through the white pages of this dissertation with the sun on your face, do not be troubled. For this is only the beginning, and you're already accompanying me through years of blood, sweat, and tears distilled into one document*. If this journey begins with the dissatisfaction of not finding your name amongst those previously mentioned, please forgive my oversight. Regardless, thank you for your kind willingness to read this dissertation.

*(adapted from the 2000 motion picture, "Gladiator").

PREFACE

This dissertation contains several chapters that are formatted as journal articles. Chapter 3 is an article entitled "Optogenetic gRNA Expression for Spatiotemporal Control of Orthogonal CRISPR/Cas Systems" that is being prepared for submission to *Nature Biotechnology*. Chapter 4 is an article entitled "Air Gap Electrospun Templates with Blue Light Gradient for Engineered Cell Stimulation" that is being prepared for submission to *Bioengineering*. Chapter 5 is formatted as a journal article that has not yet been completed, but is being prepared for submission to *Tissue Engineering – Part A*.

The work presented in this dissertation was supported by Karolinska Institutet, the Whitaker Foundation International Program Summer Grant, and the FedEx Institute of Technology Development Grant. Research reported in this dissertation was supported by the National Institute of Arthritis and Musculoskeletal and Skin Diseases of the National Institutes of Health under Award Number F31AR072502. The content is solely the responsibility of the authors and does not necessarily represent the official views of the National Institutes of Health.

ABSTRACT

Spatiotemporal organization and regulation of genomic and epigenomic processes is a phenomenon central to life. The pursuit of knowledge about these processes often requires specialized tools to be able to dissect biological mechanisms. CRISPR/Cas has emerged as a powerful tool for genome engineering, and has seen widespread use. Coupling CRISPR/Cas systems with tools that allow for spatiotemporal control is predicted to be transformational to the ability to perturb systems and gain the insights necessary to understand a diverse set of biological questions, and ultimately treat some of the most pervasive and elusive diseases. This dissertation describes the development of an optogenetic system to harness the full potential of CRISPR/Cas systems. To this end, we present BluVIPR, a system to control guide RNA production for precise spatiotemporal control of orthogonal CRISPR/Cas systems. We make special emphasis on the versatility of the system, and the compatibility with current mouse models that are stalwarts of biomedical research. We then show a proof of concept study for the delivery of light gradients to cells engineered with the BluVIPR system via air gap electrospun templates, envisioning how biomaterial-guided optogenetics could be used as a therapeutic strategy for interfacial tissue engineering. We finally show how the versatility and orthogonality of BluVIPR would allow for the development of a synthetic gene regulatory network, composed of a simple, genetically-encoded, digital demultiplexer circuit, to interpret light gradients as a cue for opposing gradient production of growth factors. We believe that this optogenetic CRISPR/Cas system is an important contribution to the toolkit of diverse biological fields of research, and envision many exciting applications in tissue engineering, tumor immunology, developmental biology, and beyond.

Table of Contents

LIST OF FIGURES

KEY TO SYMBOLS OR ABBREVIATIONS

ABE Adenine base editors

Acr antiCRISPR proteins

ASC adipose-derived stem cells

BAC Bacterial artificial chromosome

BMP-2 bone morphogenetic growth factor-2

Cas CRISPR associated protein

CBE Cytosine base editors

CMV cytomegalovirus

CRISPR Clustered Regularly Interspaced Short Palindromic Repeats

crRNA CRISPR RNA

dCas9 nuclease deficient Cas9

DSB double stranded break

ECM extracellular matrices

GRN gene regulatory network

gRNA Guide RNA

HDR Homology-directed repair

HTH helix-turn-helix

indels insertions or deletions

KRAB Krüppel-associated box domain

LOV Light-Oxygen-Voltage sensing domains

MSC mesenchymal stem cell

nCas9 nickase Cas9

NHEJ nonhomologous end joining

PAM protospacer adjacent motif

PDGF-β Platelet derived growth factor B-chain

Pip Pristinamycin-induced protein

rtTA reverse tetracycline repressible transactivator

SCN Suprachiasmatic nucleus

Scx Scleraxis

shRNA short hairpin RNA

SP Cas9 *S. pyogenes* Cas9

TetR Tetracycline repressor

TGF- β transforming growth factor-β

tracrRNA Transactivating CRISPR RNA

tTA tetracycline repressible transactivator

UGI Uracil DNA glycosylase inhibitor

UNG Uracil N-glycosylase

VP16 Herpesvirus transactivation domain

PCL polycaprolactone

HFP 1,1,1,3,3,3 hexafluoro-2-propanol

SEM scanning electron microscopy

CHAPTER 1

INTRODUCTION

Investigation of continuously fluctuating biological processes, and the subsequent desire to develop therapeutic avenues from these findings, frequently necessitates the use of tools that allow precise regulation of genomic and epigenomic features in a spatiotemporal fashion. The ability to control the cellular transcriptome, genome, and epigenome allows the researcher to create models to interrogate function and relationships, and ultimately identify key elements. The ability to control these cellular features in a manner that is defined by predetermined time and space constraints allows for the model to resemble more closely the intricate and fluid states of biological systems. Despite the importance of tools that could dissect the "where" and "when" of biological phenomena, flexible, reversible, and multifunctional tools are not currently abundant. Optogenetics has been one such tool that has seen widespread use in neuroscience, enabling the precise spatiotemporal control of neurons, especially through the use of Channelrhodopsin-2 light-sensitive ion channels[1]. Light is especially well-suited for spatiotemporal regulation of events, as it is easily focused on a desired location, and can be switched on and off in a precise temporal pattern. The success of neuronal control through light has motivated the translation of similar tools to other fields of biology, where the regulation of transcription, both for transgenes and endogenous genes, has been a main target[1–4].

The introduction of transgenes, and the precise modification of transcriptome, genome, and epigenome in cells and organisms has been a major endeavor in itself. Recent advances have made genome engineering more accessible to laboratories worldwide, accelerating research and enabling rapid generation of complex models. The genome engineering field experienced a

paradigm shift when Clustered Regularly Interspaced Short Palindromic Repeats (CRISPR) systems were adapted for RNA-guided editing of eukaryotic genomes. The CRISPR toolkit has been expanded by discovery of divergent CRISPR systems, mutation of the CRISPR associated proteins (Cas) and by addition of effectors that endow the system with diverse functions, including transcriptional activation and repression, base editing, genomic labeling, among others[5]. In the pursuit of spatiotemporal regulation of cellular functions, CRISPR-based optogenetic tools have been developed to enable control of CRISPR/Cas systems with light. These CRISPR optogenetic tools are predominantly constructed with dimerizing elements that fuse split Cas, or fuse effectors to Cas in response to light[3,6–9]. This Cas-centered approach limits the flexibility of current optogenetic CRISPR tools, as they require protein engineering, are mostly limited to transcriptional activation/repression, and are not compatible with existing CRISPR resources (such as commercially available CRISPR mice).

The overarching goal of this project was to develop an optogenetic CRISPR tool that is flexible (allowing use of all available CRISPR functionalities), orthogonal (allowing use of different CRISPR systems, separately or concomitantly), and compatible with existing CRISPR resources. Additionally, an example of how this tool could be utilized for precise control of growth factor production in tissue engineering applications was explored.

This chapter presents a succinct overview of the importance of spatiotemporal control of cellular processes, strategies to regulate these processes, CRISPR/Cas tools, optogenetic tools, and enthesis tissue engineering approaches. Ultimately, all the aforementioned aspects will provide the backdrop to the work presented in this dissertation.

TIME AND SPACE IN BIOLOGICAL SYSTEMS

Living systems have the inherent ability to maintain stable conditions in unstable environments, requiring adaptive mechanisms in constant flux and interconnection[10]. This tendency towards stability has been termed homeostasis or homeorhesis, with the former describing a system in steady-state, whereas the latter describes a system that returns to a dynamic tendency or path[11]. The coordinated effort that is required to maintain equilibrium in a multilevel organic system is complex, varying through space and time, and has been mathematically modeled by multiple researchers[12,13]. Cells adapt to their environment and maintain stable conditions through processes that are centered in the expression of genes (proteins), and this is in turn regulated by complex automatic control systems involving epigenetic, genetic, and posttranslational machineries[14]. Cybernetics, a term used to describe the communication and automatic control systems in living things and machines, was first coined by Wiener[15]. Cybernetic features have been described and modeled to understand underpinning biological mechanisms, ranging from communal to molecular scales in multilevel living systems[16–19]. With these models, researchers have attempted to dissect a multitude of mechanisms, such as metabolic homeorhesis of *S. cerevisiae* and Tumor Necrosis Factor orchestration of cellular functions in diverse modes of action[18,19]. A directing constant in these models is that organization and interpretation of signals by living systems require precise spatiotemporal control of cues and responses to these cues. In the following paragraphs, a few examples of this spatiotemporal regulation will be presented, focusing on embryonic development and biological clocks.

It is not surprising that the term homeorhesis was coined by Waddington in the context of cellular differentiation and morphogenesis in embryonic development[14]. The adhesion

to developmental paths (chreods), despite changes in the environment, is a hallmark of embryonic development that gives rise to complex multicellular organisms and specialized tissues from an unicellular origin[11]. Germ layers arising from asymmetric cell divisions establishing somatic and germline founder cells in the *C. elegans* embryo show distinctive spatiotemporal gene expression profiles, and these have been used by Hashimshony et al. to elucidate the evolutionary appearance of the germ layers[20]. It is also through spatiotemporal differential gene expression that left-right asymmetry originates in the developing embryo, as evidenced by the role of Rho signaling on the opposing sides of the primitive gut tube, described by Morckel et al.[21]. Furthermore, Meyer et al. described branching of epithelial tubes as a consequence of spatiotemporal control by morphogenetic molecules in the developing kidney[22]. It should be apparent that spatiotemporal regulation is a major contributor to embryonic development, and can be implicated in many more developmental phenomena than the selected examples above. It is also interesting to ponder on how the spatiotemporal regulatory cues presented to the embryo are themselves regulated in a spatiotemporal fashion, involving multiple overlaid cybernetic feedback loops. The sequence of early reproductive events from folliculogenesis to blastocyst implantation require coordinated and spatiotemporally regulated endocrine, paracrine, and autocrine communication[23]. The interpretation of signaling cues and subsequent responses in the early and developing embryo involve direct gene expression regulation through signaling cascades, chromatin interaction networks that regulate epigenetic and genetic states, spatiotemporal network structures, and liquid-like condensates directing transgenerational epigenetic inheritance[24–26]. Spatiotemporal gene regulation is also part of the directional sensing mechanisms that allow cells to exhibit chemotaxis and respond to molecular gradients to transport themselves to determined locations, enabling spatial organization of

embryonic tissues and response to injury[27]. These molecular mechanisms implicated in embryonic development are retained through post-natal timeframes in specialized responses, particularly healing responses. Fracture healing is an example, where mechanisms that regulate cell migration, differentiation, and growth are recapitulated in a spatiotemporally regulated manner to repair skeletal structures in a post-natal environment[28].

The duration of embryonic development is determined by internal biological clocks that are species-specific, and are part of one of two major classes of biological clock: hourglasses[29]. The second major class of biological clock are oscillators, and these include the well-known circadian clocks, that in mammals are a network of interconnected clocks with a central pacemaker in the suprachiasmatic nucleus (SCN) of the ventral hypothalamus, which is adjusted by light cues sensed by the retina[29]. The tissue structure of the SCN exhibits a particular spatial organization of SCN cellular oscillators, coupled in a way that allows for gene expression to set an intermediate period, integrating the signals of the individual oscillators[30]. This integrated signal is then propagated to the rest of the network, setting interdependent nodes that, in turn, regulate local events in a spatiotemporal manner[30,31]. This system of multiple autonomous, but interconnected, clocks improves adaptation to variable environments[32]. Though light is the major zeitgeber for adjusting central circadian clocks, other time keeping signals, like feeding, are important for peripheral clocks, and these set gene expression patterns that are tissue-specific (and thus spatiotemporally constrained in nature)[32,33]. The cybernetic networks of these multiple clocks, responding to multiple cues and being recalibrated in a spatiotemporal manner, sets a spatiotemporal regulator for virtually every cell in an organism[29]. Thus, from pre-implantation events to death, living systems are responding to their environment through a series of interconnected networks that maintain homeostasis and homeorhesis through spatiotemporal

regulation of molecular mechanisms central to life itself, and anchored in the central dogma of molecular biology.

Given the importance of the cybernetic nature of living things, and how spatiotemporal patterning of gene expression lies at the heart of these control systems, it follows that tools that allow for better modelling and precise perturbation of the genetic and epigenetic aspects of the systems, to dissect component function and causal relationships, are highly desirable. Balling expresses this desire very well: "Imagine titrating the expression of single genes in specific cell populations at will"[34]. Armed with the information about networks and biological dynamics that these tools will facilitate, the ability to understand and eventually modulate complex biological systems for therapeutic aims will grow significantly[34].

TOOLS FOR SPATIOTEMPORAL GENOMIC AND EPIGENOMIC REGULATION

In the pursuit of spatiotemporal regulation of genomic and epigenomic structures and processes, researchers have developed an ever-growing arsenal of tools and techniques. The following sections will provide a succinct overview of common approaches to inducible genomic and epigenomic engineering, giving context to, and providing the foundations of, the work presented in this dissertation.

TEMPORAL REGULATION

Inducibility of gene expression at a determined time point allows researchers to study genes that are toxic when expressed constitutively or in particular stages of development, and can give rise to the opportunity to observe the effect of gene expression by presenting clear "before" and "after" scenarios[35]. Conversely, inducible gene repression expands the toolset by presenting loss of expression in a precisely time-determined manner. To date, most inducible expression or repression systems rely on small molecules as effectors[35–40]. The first widely

available inducible gene expression system to be developed was the Tet-Off system[41]. In this system the tTA transactivator is created by fusing the *E. coli* tet repressor (TetR) with the herpesvirus transactivation domain VP16[36,41]. The presence of tet operator DNA sequences upstream of a target gene and a minimal promoter allows the binding of tTA and subsequent transcription of the downstream sequences[41]. Tetracycline binds tTA, blocking DNA binding domains and abolishing transcription[41]. A mutated form of tTA, termed reverse tTA (rtTA), binds DNA only in the presence of tetracycline or its analogues, effectively reversing the stimuli responsiveness of the inducible expression system, creating a Tet-On switch[36]. These systems, Tet-On and Tet-Off, allow precise regulation of gene expression upon addition of tetracycline or its analogues (i.e. doxycycline), present relatively low basal levels of expression (leakiness), and potent activation (dynamic range)[35,36]. Due to the convenience and cost effectiveness of doxycycline administration, and good bioavailability when used *in vivo*, Tet-On systems in particular have seen widespread use in diverse fields of biology[36]. Alternative approaches using the same allosteric strategy utilize steroids, like ecdysone (from *Drosophila*) or a mutant human progesterone receptor that only binds progesterone antagonist RU486[35,36,42]. In both of these systems, DNA binding domains are fused to VP16, activating the gene downstream of the recognition elements and minimal promoter in a drug-inducible manner[36,42]. Similarly, PipOFF and PipON systems rely on fusion transactivators derived from the repressor pristinamycin-induced protein (Pip) to regulate gene expression under stimulus of streptogramin antibiotics[37]. These drug-inducible gene expression tools have been very useful for the precise regulation of transgene expression in a temporal basis, but researchers have also developed tools based on drug-inducible promoters to target (and silence) endogenous genes. For example, Kappel et al. described a system in which an H1 promoter expresses short hairpin RNA (shRNA) under the

control of tetracycline[39]. Similarly, Gupta et al. developed a U6 inducible promoter that expresses shRNA under the control of ecdysone[38].

An interesting addition to the toolkit aimed at temporal regulation of gene expression is the utilization of heat shock protein promoters to activate transcription when cells are exposed to elevated temperatures (42°C)[43,44]. These systems utilize native cellular responses, mainly heat shock protein 70 upregulation, that regulate gene expression patterns to protect the cell from elevated temperatures[43]. Yang et al. have described a system that uses a heat shock promoter to drive microRNA mimics, targeting and silencing endogenous targets[45]. The potential off target effects of activating the heat shock pathway in an experimental or therapeutic setup are concerns when using this system. Of note, this system can be combined with focused ultrasound to generate precise spatial regulation of gene expression, in addition to the temporal regulation aspect already discussed[43].

SPATIAL REGULATION

The phenotype of a multicellular organism arises when differential gene expression is orchestrated in a precise spatiotemporal manner[46]. The mechanisms that regulate this cell lineage-specific differential expression are therefore extremely important research targets, but they are themselves a tool to limit expression of a gene of interest to specific cells or tissues, bringing spatial control to transgene expression[46–48]. In its simplest form "transcriptional targeting" through tissue-specific differential expression places a transgene downstream of the tissue-specific promoter of choice[49]. Efforts to map these tissue-specific regulatory elements have yielded a number of identified genes whose promoter is differentially activated in a cell or tissue-type discriminating manner[50]. Thus, once a researcher has identified the adequate tissue-specific promoter, the gene of interest is cloned downstream of a copy of the regulatory element

for this promoter and the differential expression innate to the biological system ensures that the gene of interest is expressed in the desired tissue. Examples of this approach have targeted hematopoietic cell lineages through CD43, neurons through platelet-derived growth factor B-chain (PDGF-β), and endothelial cells through TIE2, among others[51–53]. The major limiting factor when using simple transcriptional targeting as described above, is that robust transcription is seldom achieved, limiting the dynamic range of expression for the gene of interest[47,52,54]. Low transcription levels have been tackled in multiple ways, mainly by adding enhancers or transactivators to the native tissue-specific regulatory elements and transcription factor; or by utilizing site-specific recombination strategies (like the Cre-Lox system). Liu et al. placed cytomegalovirus (CMV) enhancers upstream of PDGF-β promoter sequences to improve transcriptional levels of transgene expression in neurons[52]. Other groups have attempted to boost transcription through the coupling of transactivation domains (VP16, p65, etc) to either the native tissue-specific transcription factor protein, or to xenogeneic transactivator fusions (Gal4, tTA, etc) that are regulated by the endogenous tissue-specific promoter and then bind regulatory elements of the transgene, driving robust transcription[53,55–57]. It is important to note that these strategies using inducible transactivator fusions also confer temporal regulation of the transgene, as seen in the previous section. In a parallel approach, the Cre-Lox site-specific recombination system can be used to remove a Lox-flanked stop cassette in the transgene, effectively activating transcription and translation of the gene of interest[58]. To limit the activity of the Cre recombinase to specific tissues, the sequence encoding the recombinase is placed under tissue-specific promoter regulation[48,54]. In this strategy, the promotor driving the transgene can be constitutively active or inducible, hence allowing for the possibility of temporal control of transcripts that are only successfully translated in a spatially-restricted fashion[59]. Furthermore, all of the strategies

for transcriptional targeting described thus far can be assembled in complex arrays with specific enhancers and large genomic regions, then delivered in bacterial artificial chromosomes (BAC) to further expand the toolset[47].

Spatial regulation of gene expression through means that are not dependent on tissue-specific transcriptional targeting have also been explored, using physicochemical cues to initiate transcription. Madio et al. described the use of magnetic resonance imaging (MRI) guided focused ultrasound to precisely elevate temperature at a desired location and activate gene expression through heat shock response[43]. Ausländer et al. developed synthetic gene regulatory networks to control gene expression in response to pH and CO_2 levels in mammalian cells[60]. While other groups have recognized the inherent advantages of using light as a spatiotemporal regulator, and these strategies will be further discussed in a latter section of this introduction.

It should be clear that a fundamental concept of spatiotemporal regulation of gene expression is that of targeting a particular regulatory element with a transcription factor (or transactivator fusion that binds the regulatory element). This bipartite system then allows for the organization of one or both of the required elements in a fashion that is spatiotemporally restricted. An exciting tool that has revolutionized genome engineering in the last decade, CRISPR/Cas, is a bipartite system that can be targeted to specific genomic locations, thus making it an ideal candidate for development of spatiotemporal regulatory systems of gene expression.

CRISPR/CAS

CRISPR arrays were first noted as anomalies in prokaryotic genomes and subsequently identified as primitive bacterial and archaeal acquired immune systems[61]. In its essence, CRISPR/Cas is an RNA-guided restriction machinery, aimed at identifying and destroying

previously encountered mobile genetic elements, such as plasmids, transposons, and bacteriophages[61,62]. The sequences that lie in between the regularly interspaced palindromic repeats are known as spacers, and are foreign genomic sequences that have been integrated into the bacterial genome[62]. These sequences are transcribed into RNA and used as a guide to direct Cas proteins to degrade invading foreign nucleic acids[61,62]. The ribonucleoprotein complex of Cas and CRISPR RNA scans nucleic acid sequences and checks for complementarity to the spacer when a protospacer adjacent motif (PAM) is recognized[61]. If this complementarity exists, nuclease domains in the Cas protein cleave the foreign nucleic acid[61,62]. This two component system has been engineered to function in eukaryotic organisms, targeting genomic sequences by easily manufactured RNA sequences, greatly improving the ease of genome engineering[62]. The diversity of CRISPR/Cas systems and the efforts to classify these will be discussed in a following paragraph of this introduction.

The first adaptations of CRISPR/Cas for eukaryotic genome engineering centered around *S. pyogenes* Cas9 systems (SP Cas9)[61,62]. In the native SP Cas9 system, the RNA directing DNA cleavage is transcribed in two separate parts: CRISPR RNA (crRNA) and trans-activating CRISPR RNA (tracrRNA)[61]. The crRNA:tracrRNA duplex is combined into a single synthetic chimeric transcript in engineered versions of the SP Cas9 system, and termed guide RNA (gRNA)[61]. These gRNAs are designed to include an 80bp scaffold that interacts with Cas9 (specific to SP Cas9) and a 20bp targeting portion, that should be complimentary to the intended target[61,62]. The target should be flanked on its 3' end by a PAM specific to SP Cas9, NGG[61,62]. When coupled to this gRNA, SP Cas9 is activated, and the PAM recognition domain is available to recognize the three nucleotide sequence flanking the target. Once this PAM is recognized, RuvC and HNH domains are activated, generating double stranded breaks (DSB) at the target

site[61]. These DSBs are repaired by cellular DNA repair mechanisms, predominantly by the error-prone nonhomologous end joining (NHEJ) mechanism, allowing for the introduction of small mutations (insertions or deletions (indels)) at the target site[61,62]. Typically, one nucleotide insertions are predominant, followed by one nucleotide deletions as the most common indels. These indels cause frame shift mutations, effectively abolishing the correct translation of the target gene, generating a knock out[61]. If a template DNA that includes flanking sequences homologous to the sequences adjoining the target DSB, the cell will also repair DNA through a process known as homology-directed repair (HDR). The template DNA then serves as both a guide for the repair mechanism, and a vehicle for introducing a new sequence into the genome, generating knock-ins[61]. This nuclease activity of SP Cas9 has seen widespread use, and is the source of the popular nickname for CRISPR/Cas systems: "gene scissors".

Engineered point mutations in the RuvC or HNH domains of Cas9 abolish nuclease activity, enabling the generation of a nickase Cas9 (nCas9),generating single strand breaks, if only one domain is mutated, or a nuclease deficient Cas9 (dCas9) if both domains are mutated[61]. These mutated versions of Cas9 can be fused to different effectors, conferring various functionalities to the Cas9 system[61,63–67]. Targeting sequences downstream of promoters with dCas9 represses transcription, presumably by steric hindrance, but when fused to an effector that functions as an epigenetic transcription repressor (like Krüppel-associated box domain (KRAB)), TRIM28 and associated chromatin remodeling machinery are recruited, strongly silencing the target gene[64,65]. This strategy of CRISPR/Cas-guided gene repression is known as CRISPRi. Conversely, if one targets a region upstream of a promoter and uses a dCas9 fused to transactivation domains (like VP64, p65, Rta, HSF1, etc), transcription machinery is recruited and the target gene is expressed[61,63,65]. This mechanism is known as CRISPRa. These

transactivation domains can be combined to form synergistic CRISPRa synthetic transcription factors, like dCas9-VPR (VP64, p65, and Rta), and achieve robust activation of target gene transcription[68]. If an nCas9 is fused to a deaminase enzyme, precise single point mutations can be introduced or reversed in the targeted genomic sequence[66]. These base editors are classified into two main classes: Adenine base editors (ABE) and Cytosine base editors (CBE), depending on the target nucleotide to be edited[66,67]. ABEs convert an A:T base pair into a G:C base pair, while CBEs convert a C:G base pair into a T:A base pair[66]. CBEs include a cytidine deaminase that removes an amine from the target cytosine, generating uracil, which is read as a T by the DNA polymerase involved in the repair of the single stranded nick created by nCas9[66]. The intermediate U:G base pair generated by C deamination is quickly repaired by cellular mechanisms, primarily employing uracil N-glycosylase (UNG) and reversing the editing event before complete repair of the nick is completed, lowering editing efficiency dramatically[66]. To overcome this, CBEs can incorporate an uracil DNA glycosylase inhibitor (UGI), which is a DNA mimic that strongly inhibits UNG activity and allows the completion of C to T editing[66]. ABEs function in an analogous manner, but employ a deoxyadenosine deaminase that was evolved from a tRNA adenosine deaminase enzyme from *E. coli*[66]. Thus, adenine is converted into inosine, read as G by polymerases. Cells have much less ability to remove inosine from DNA, compared to uracil, so the use of UGIs is not necessary with ABEs[66].

The CRISPR-based genome and epigenome engineering tools that have been described this far are all centered around SP Cas9. The CRISPR/Cas system is present in many bacteria and archaea, and considerable efforts have been set forth to identify and classify the numerous types of systems[69]. This task is non trivial, mainly because the CRISPR arrays vary and don't contain enough information for accurate identification and classification, and because Cas

proteins and the associated modules are frequently shuffled and varied[69]. CRISPR/Cas systems are divided into two classes (1 and 2), each divided into types (I ,II ,etc) and subtypes(A, B, C, etc)[69–71]. Most types that have been adapted for genome engineering applications belong to class 2 systems, mainly because the hallmark of this class is the presence of a single Cas that is sufficient for DNA or RNA targeting and cleavage[69]. Each type of CRISPR system has its own functional idiosyncrasy, with differing gRNA, PAM, and gRNA processing mechanisms (even varying within species of the same type and subtype)[69–71]. This review will describe two other class 2 CRISPR systems that are used in genome, epigenome, and transcriptome engineering. Cas12a, previously known as Cpf1, is a type V, subtype A CRISPR/Cas system that targets DNA and has the ability to process gRNA without any auxiliary factors[69,72]. Cas12a systems recognize the TTTV PAM sequence, making it useful when targeting areas that are not GC rich and unavailable to Cas9[72]. The gRNA structure for Cas12a systems consist of a 5' spacer and a 3' direct repeat (DR) that forms a hairpin structure and couples with the Cas protein[72]. The four main functions (nuclease, activation, repression, and base editing) have all been developed for the Cas12a systems[73]. Altogether, the characteristics of Cas12a systems make them complementary to Cas9 systems, expanding the available target sites in the genome, and offering the capability of deploying orthogonal systems simultaneously. Cas13d is a type VI, subtype D CRISPR/Cas system that targets RNA and can process gRNA without any auxiliary factors[69,74]. The ability to target RNA makes this CRISPR type unique, and allows for targeting mRNA for gene silencing, targeting mRNA splice junctions with dCas13d to induce alternative splicing, and when fused to deaminases, targeting mRNA for base editing[66,74].

As mentioned previously, CRISPR/Cas systems evolved as adaptive immune mechanisms in prokaryotes against invading mobile genetic elements. Biological processes not

being static, the evolutionary warfare response from these invaders led to the rise of small proteins that hinder the activity of CRISPR/Cas: anti-CRISPR proteins (Acr). There is a tremendous variety of Acr, with more than 20 different families described to date[6]. These Acr have evolved to be highly specific and have great affinity for their targets[6]. The small size and effectiveness of Acr have made them an attractive target for adding functionalities and limiting Cas9 activities in a spatiotemporal manner[6]. More details of Acr and uses in spatiotemporal regulation of CRISPR/Cas systems will be presented in chapter 5.

CRISPR/Cas systems have revolutionized the genome engineering field and their bipartite nature (when using class 2 systems) lends itself to the possibility of combining expression systems previously discussed for spatiotemporal regulation. Perhaps the most exciting stimulus for generating precise spatiotemporal regulation is light. CRISPR/Cas systems have been combined with optogenetic tools successfully. A brief overview of optogenetic tools and the current optogenetic CRISPR/Cas toolkit will be presented in the following section.

OPTOGENETICS

Light is relatively inexpensive, highly controllable in both space and time, has minimal untargeted effects on cells, can be dose adjustable by varying intensity, and, depending on wavelength, can have different tissue penetration properties, and activate different light-responsive components. It is due to these characteristics that light has long been a tool for targeting cellular and molecular mechanisms when high spatiotemporal control is required[75]. First attempts to stimulate neurons directly with lasers date back to the 1970s, with various strategies involving fluorescent proteins, genes in combinations with chemicals, and photocaged ligands, among others, used with varying degrees of success[75]. The advent of single-component optogenetic tools, notably microbial opsins, permitted the fast development of optogenetics

during the past 15 years, allowing for delivery of genetically-encoded optogenetic tools for complex experiments[75,76]. The first microbial opsin to be adapted to optogenetic stimulation of neurons was a channelrhodopsin, used in hippocampal neurons by Boyden et al.[75,77]. These single component, genetically-encoded optogenetic tools enable highly precise spatiotemporal regulation, and require no other external chemicals or stimuli other than light[75]. In comparison with optogenetic tools that depend on photocaged or photolabile chemicals, genetically-encoded optogenetic tools are often more economical, do not diffuse, are reversible (on/off switching), and are easier to deliver to certain cell populations[78]. These advantages have propelled opsin-based optogenetic tools to widespread use, particularly in the fields related to neuroscience[75,78]. Applications range from studies on basic neuronal networks to disease-oriented investigation, for example in epilepsy, depression, spinal cord injuries, etc[79–83]. These tools have been employed in *in vitro* and *in vivo* studies, allowing for precise interrogation of neuronal function even in freely-moving mammals[75,82,84]. While the fields related to neuroscience have benefited from the advent of these optogenetic tools, fields that deal with excitable, depolarizing tissue have also adapted tools for their particular needs, as evidenced by experiences in cardiac optogenetics[85].

As was discussed in previous sections of this introduction, spatiotemporal patterning plays a crucial role in embryonic development. Thus, developmental biologists have adapted and used optogenetic tools[86]. For non-neuronal optogenetics, microbial opsins and related tools have limited functionality, therefore it was the adaptation of cryptochrome, phytochrome, and light-sensitive proteins for optogenetic perturbations that carved a path to utilities within other fields[86]. Light-sensitive proteins that do not require addition of foreign chromophores are particularly important tools, as they are then single component, genetically-encoded optogenetic tools[86]. Light-Oxygen-Voltage (LOV) sensing domains are particularly interesting, as they undergo

reversible, light-mediated conformational changes that enable protein-protein and protein-DNA interactions[86,87]. The allosteric function granted by the interactions with protein domains or nucleic acids has allowed this toolset to create nuclear import, signaling cascade, and transcription regulation optogenetic tools[86,88–90].

EL222 is a protein from *E. litoralis* in which an LOV domain binds and inhibits a helix-turn-helix (HTH) DNA binding domain in dark state, and releases the HTH under blue light (470nm wavelength), allowing it to bind DNA (Figure 1)[89]. The chromophore for EL222 is flavin which is present in eukaryotic cells, enabling use of EL222 in mammalian cells, including human[89,90]. The recognition elements, DNA sequences in the bacterial genome, that EL222 HTH binds to have been identified, and analogous sequences have been placed upstream of a minimal TATA box promoter to enable the use of an VP16-EL222 fusion to act as a synthetic transcription factor and drive expression of a transgene[90]. This strategy is depicted in chapter 3, Figure 3. EL222 has been successfully used in mammalian cells, *in vivo* in zebrafish, and even to drive Cas9 expression to enable optogenetic control of CRISPR/Cas nuclease function[90,91]. As the VP16-EL222 system was one of the foundations for the work presented in this thesis, more details about this tool will be discussed in chapter 3.

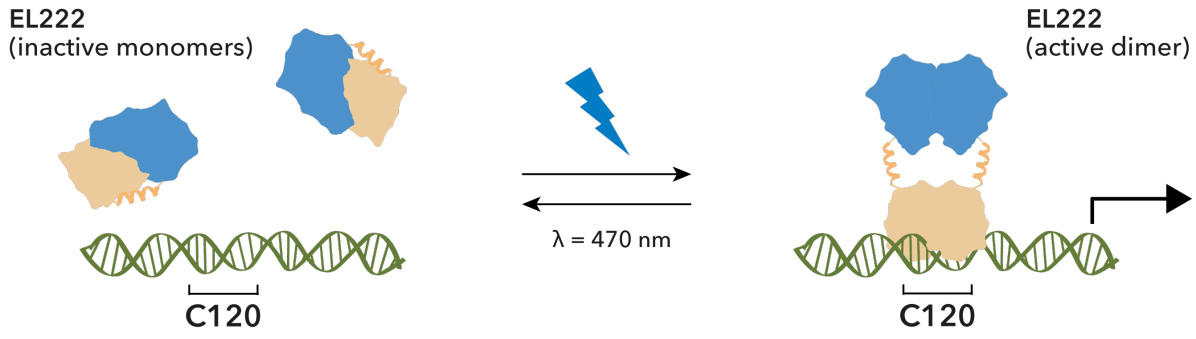

Figure 1: Schematic representation of EL222 monomers in dark state, and their dimerization under light stimulation. The dimerization exposes the HTH domain, allowing the dimer to bind DNA. C120 is the engineered, repeated recognition element.

LOVs and other light-activated dimerization strategies have been employed in the pursuit of optogenetic CRISPR/Cas tools, beyond the previously discussed example with EL222. A common trait is that most reported strategies to date have focused on the Cas protein portion of the CRISPR/Cas system. Approaches in which the Cas protein is split and each half is fused to photo-activatable dimerizing domains have been successfully used by several groups[6]. Other tools have fused dimerizing domains, particularly cryptochrome domains, to a dCas9 and an effector (e.g. transactivation domains, like VP64), like the LACE system by Polstein et al.[3]. The use of light-induced dimerization domains that would sterically hinder the DNA binding cleft of Cas have also been explored[6,7]. While successful, these Cas-centered approaches require protein engineering of the Cas itself, limiting orthogonality and the use of off the shelf transgenic animal models. The few attempts at regulating gRNA-centered optogenetic control of CRISPR/Cas have revolved around caged or otherwise chemically modified gRNAs that gain function upon light exposure[6,8,9]. These systems are limited by the need of introducing chemically modified gRNAs, a non-trivial task in *in vivo* models. This dissertation describes the development of a gRNA-centered optogenetic CRISPR/Cas tool, using EL222, in chapter 3.

As the use of non-neuronal optogenetic tools have increased in basic research, the cross-over of these tools to synthetic biology and possible therapeutic avenues has begun. One example is the work by Ausländer et al., where optogenetic gene regulatory networks (GRN) in cellular implants for diabetes treatment have been explored[92]. As a showcase of the potential uses of a CRISPR/Cas optogenetic tool that could integrate orthogonality, biomaterial-mediated optogenetic synthetic biology, anti-CRISPR proteins, and precise spatiotemporal regulation for

morphogenetic gradient formation, this dissertation describes tissue engineering of the enthesis as an example application in chapters 4 and 5.

EXAMPLE APPLICATION

In the USA alone, more than half of the 100,000 people that undergo anterior cruciate ligament reconstruction surgery and nearly 80 percent of the 500,000 that have rotator cuff repairs every year will experience repair failure, mostly due to the current inability to regenerate a properly functioning enthesis[93–96]. High failure rates lead to significantly increased cost and time to recovery[93]. The specialized interface referred to as the enthesis, the insertion of tendons/ligaments into bone, is a highly-organized tissue presenting continuous gradients of structural and mechanical properties that allow smooth force transfer, protecting and maintaining the tendon/ligament insertion (Figure 2). The lack of regeneration of the enthesis leads to high failure rates after these procedures due to formation of a discrete transition of tissue characteristics which acts as a force concentrator that, under mechanical loading, is the site of rupture[93,96]. The clinical importance of regenerating the natural structure of entheses have made them a recent focus of tissue engineering, with the generation of smooth mechanical and structural gradients still a major challenge. The enthesis is divided into four zones with extracellular matrices (ECM) and cell types varying in a smooth gradient fashion [93]. The first zone of the enthesis is the tendon/ligament proper, characterized by parallel collagen type I fibers, arrays of elongated fibroblasts, and proteoglycans[94]. This zone has mechanical properties similar to those of the tendon/ligament[95]. The second zone is uncalcified fibrocartilage with round fibrochondrocytes arranged in rows surrounded by ECM composed of aggrecan and collagen types I, II, and III [93]. This zone is avascular and functions as a force damper, dissipating stress generated by bending collagen fibers in the tendon[93]. The third zone is avascular, calcified

fibrocartilage with hypertrophic fibrochondrocytes and ECM composed of aggrecan and collagen types II and X[93,94]. The third zone is at the boundary with subchondral bone and is highly irregular, providing mechanical integrity through the attachment of the mineralized layer to the bone[93]. Some studies suggest that this zone is important for blocking blood supply from reaching the avascular zones in the enthesis and tendon/ligament, preventing communication between the compartments[93]. The fourth zone is the bone proper, characterized by populations of osteoblasts, osteoclasts, and osteocytes residing in a disorganized ECM of type I collagen and hydroxyapatite[93].

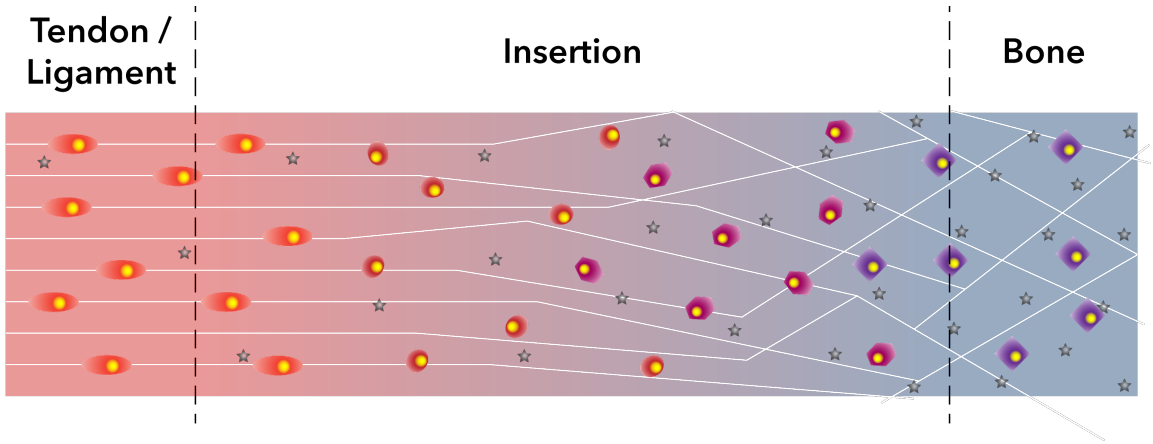

Figure 2: Schematic representation of the enthesis, depicting the different zones and the gradients of cells, extracellular matrix, and signaling molecules exhibited in the transition from tendons/ligaments to bone tissues.

Though the four zones exhibit clear compositional and functional differences, it needs to be stressed that the structure is continuous and the gradient contributes greatly to the function of the tissue[93–96]. The development of these zones occurs postnatally, although the exact process is poorly understood. A combination of physicochemical stimuli drive the gradient formation in the interfacial structure[94–96]. Transcription factors Sox9 and Scleraxis (Scx) play important roles in the development of the enthesis, and are arranged in countergradient fashion in immature

postnatal entheses[94]. Scx is associated with tenogenesis, while Sox9 is widely accepted to drive chondrogenesis. The primitive enthesis is composed of a pool of progenitor cells that express both transcription factors (Scx+/ Sox9+), and progressively polarizes to include a pool of Scx-/Sox9+ and Scx+/Sox9- cells[94,96]. The development of the Scx and Sox9 countergradient is believed to be stimulated by transforming growth factor-β (TGF-β) as well as mechanical forces acting on the enthesis[95]. These stimuli are both present during healing responses, but it is not yet understood why the result is fibrous scar tissue without the functional structure of the enthesis[94,96]. Several studies have focused on the use of other growth factors for enthesis regeneration, with platelet-derived growth factor (PDGF) and bone morphogenetic growth factor-2 (BMP-2) garnering great attention[97–101]. PDGF-B has been associated with ligament/tendon regeneration both in vitro and in vivo[97–99]. BMP-2 has been widely used for bone regeneration[97,100,101]. Both growth factors have been FDA approved for clinical use, and in a preclinical study where a gradient of BMP-2 and PDGF-B was immobilized in a porous membrane, they directed mesenchymal stem cell (MSC) differentiation in vitro to recreate gradient structures[97]. While this study is promising, the use of recombinant proteins presents several challenges: high cost, handling difficulty, supraphysiological dosages, and less effectiveness than paracrine, endogenous stimulation. The adult enthesis has no native populations of stem cells in the tendon/ligament portion, but the presence of osteoblastic precursors is evident in the bone zone[96]. This lack of stem cells and the poor vascularization of the enthesis zones 1-3 partially explain the lack of proper healing[95]. Most current studies that focus on cell-based strategies for enthesis regeneration use MSCs (bone marrow and adipose-derived) due to their relative abundance, ease of expansion, and ability to differentiate into the cells that populate the native enthesis[93–96].

A potential optogenetic tissue engineering strategy is presented in which an electrospun template (component 1) will be used to deliver physicochemical cues to engineered cells (component 2) to generate an opposed gradient of growth factors that will guide the regeneration of the structural and functional characteristics of the enthesis. To accomplish this goal, engineered cells with synthetic gene regulatory networks constructed with CRISPR-based logical gates, respond to the stimuli presented by the template. Details regarding this strategy are presented in chapters 4 and 5.

In this dissertation, the successful development of an optogenetic CRISPR/Cas tool that unleashes the full functionality of the CRISPR toolset will be described. Furthermore, the development of air gap electrospun templates that can deliver gradients of blue light to cells for spatiotemporal regulation will be discussed. Finally an optogenetic synthetic biology approach incorporating both of the elements defined above will be proposed, and preliminary work leading to this goal will be presented.

CHAPTER 2

SPECIFIC AIMS AND MOTIVATION

The purpose of this work was to develop a novel system for optogenetic control of CRISPR/Cas systems that enables precise spatiotemporal regulation of any Cas and relevant functional variants, and to showcase the versatility and utility of such a system through a novel strategy for morphogen gradient production for tissue engineering of the enthesis. It is hypothesized that a versatile, fully orthogonal optogenetic CRISPR/Cas system will enable researchers to address many important biological questions across different fields and further progress towards therapeutic interventions. To achieve this, focus was placed on three specific aims:

1. Develop an optogenetic gRNA production system and test its compatibility with different Cas9 functions, and other Cas types.
2. Investigate the potential of delivering a gradient of blue light via an air gap electrospun template.
3. Develop an optogenetic CRISPR/Cas-based digital demultiplexer circuit to enable the generation of opposing gradients of BMP-2 and PDGF in response to physicochemical gradients for tissue engineering of the enthesis.

CHAPTER 3

OPTOGENETIC gRNA EXPRESSION FOR SPATIOTEMPORAL CONTROL OF ORTHOGONAL CRISPR/CAS SYSTEMS

CRISPR/Cas has emerged as a powerful and versatile system for controlling gene activity and introducing precise mutations in the genome[62,102,103]. The original CRISPR/Cas system used for programmable DNA cleavage is based on type II Cas9 from *S. pyogenes*, and has now been supplemented with Cas proteins from other bacterial species (e.g. *S. aureus* and *E. coli*) and of other types (e.g. Cas12, Cas13)[70,71]. The use of orthogonal Cas proteins may have several advantages, including expanded target space due to alternative protospacer adjacent motifs (PAM), targeting of RNA, and decreased size for more efficient viral delivery (SaCas9 or LbCas12a). Importantly, spatiotemporal control of CRISPR/Cas activity addresses a level of control necessary for exploration of new biological questions, and could be useful in future therapeutic settings to limit unwanted CRISPR/Cas activity and regulate genomic and epigenomic events in a precise manner[78,88,104]. Most current methods for spatiotemporal control of CRISPR/Cas systems are based on light-induced dimerization of split-Cas, or dimerization of Cas with effectors[3,6,7]. To expand the use of light-induced split-Cas systems to additional functions, species, and types of Cas, e.g. base editors and Cas13, therefore requires cumbersome engineering of new split-Cas variants. Furthermore, the availability of discrete and orthogonal dimerizing domains is limited, further complicating the use of multiple Cas functions in a single cell, which is desirable when constructing closed loop and synthetic gene regulatory network systems.

To avoid the limitations of current split-Cas systems we have generated an optogenetic platform for light controlled expression of gRNA, allowing for complete spatiotemporal control, multiplexing and full orthogonality. To achieve this, we have established a system for ribozyme-dependent expression of gRNAs from a light activated RNAPII promoter. This allowed us to control the activity of several orthogonal Cas proteins, including activators, repressors, and base editors, by using blue light.

To enable light-induced activation of gRNAs we took advantage of the blue light-activated protein EL222[90]. Upon exposure to blue light (470nm), EL222 dimerizes and binds to its response elements in the C120 promoter[90]. By fusing EL222 to a transcriptional activator, blue light activation of EL222 leads to RNAPII mediated transcription from C120 (Figure 3a). To allow for the production of gRNAs from an RNAPII promoter, we flanked the gRNA sequence with hammerhead (HH) and Hepatitis delta virus (HDV) ribozymes, leading to precise excision of the gRNA sequence from the transcript (Figure 3b)[105]. To track the induction of C120 by blue light in some applications, we generated a version with an mCherry reporter between the C120 promoter and the HH-gRNA-HDV (RGR) cassette.

The current generation of EL222 activator is fused to VP16 (VP16-EL222), resulting in moderate activation of reporter genes downstream of C120 after exposure to blue light (Figure 5)[90]. Importantly, the activation of VP16-EL222 by blue light did not produce sufficient amounts of gRNA for dCas9-VPR dependent activation of endogenous genes (Figure 6). To obtain sufficient levels of gRNA transcription, we therefore replaced the VP16 activation domain of VP16-EL222 with the more potent VP64-p65-Rta (VPR) transcriptional activator, thus creating a second generation of EL222 activator (VPR-EL222) (Figure 6). We then generated a plasmid for blue light-activated universal VPR-improved production of RGRs (BluVIPR) containing VPR-

EL222, a C120 promoter, an optional mCherry reporter, and an RGR (Figure 3c). To assess how BluVIPR compared to traditional chemogenetic induction systems, we also generated a plasmid for doxycycline induced expression of RGRs (Dox-RGR). The mCherry reporter was strongly activated in both BluVIPR and Dox-RGR after exposure to blue light or doxycycline, respectively (Figure 3d). We then tested the ability of BluVIPR and Dox-RGR to induce the expression of endogenous genes through activation of SpdCas9-VPR, and found BluVIPR was as potent as Dox-RGR and with significantly lower background (Figure 3e). This demonstrated that the improved VPR-EL222 induced sufficient levels of gRNA to activate SpCas9.

In contrast to previous induced CRISPR/Cas systems, where the induction is based on chemical or light-induced dimerization of split-Cas, or of recruitment of effector domains to dCas9, the BluVIPR system allows for optogenetic control of genetically encoded, nonmodified gRNAs. One major advantage of this is that BluVIPR can be easily combined with any available Cas protein, without the need for split-Cas, recruited effector domains, or chemically modified gRNAs. BluVIPR therefore allows for e.g. light-induced base editors, and light-induced Cas13d. The BluVIPR system can also be introduced in cells from commercially available Cas9, dCas9-SPH, and dCas9-SunTag mice, simplifying light-based control of CRISPR/Cas in primary cells and readily available, off-the-shelf animal models. Furthermore, the BluVIPR system allows for multiplexed induction of several gRNAs, including induction of multiple gRNAs with different scaffolds for simultaneous activation of orthologous Cas proteins.

To prove the versatility of the system, we combined BluVIPR with SpCas9 functional variants, and Cas proteins of different types. We first tested the ability of BluVIPR to direct SpCas9 DNA cleavage. For this, we co-transfected a reporter cell line based on HEK293T cells harboring a dTomato fluorescent protein that has been mutated to be out of frame and therefore

non-functional, with an SpCas9 plasmid and a BluVIPR plasmid containing an RGR targeting a region upstream of the dTomato transcription start site (TSS) (Figure 3f). Upon blue light stimulation, Cas9 mediated cleavage is repaired and the most common indel (-1) restores the reading frame and activates dTomato (Figure 3g). Furthermore, we used BluVIPR to induce the activity of SpnCas9 base editors (Target-AID and ABEmax). HEK293T cells were used to generate C-to-T and A-to-G base editing reporter cells by insertion of a mutated start codon (C-to-T) or a premature stop codon (A-to-G) in EGFP, which would be edited to a correct start codon by Target-Aid or ABEmax and allow expression of EGFP (Figure 3h)[106,107]. After exposure to blue light, flow cytometry data shows a population of cells with both mCherry and EGFP expression, evidence of optogenetic base editing (Figure 3i). Fluorescence microscopy confirms the presence of EGFP in cells with targeting gRNA that have been stimulated by blue light (Figure 3j).

A major advantage of the BluVIPR system is the ability to use orthogonal Cas proteins of different types. To prove this, we used the BluVIPR system to activate the Type V Cas12a to activate endogenous PDGFB transcription (Figure 3k)[74]. In HEK293T cells that have been transfected with BluVIPR and stimulated with blue light, PDGFB levels are around 4-fold higher than in cells that remained in the dark.

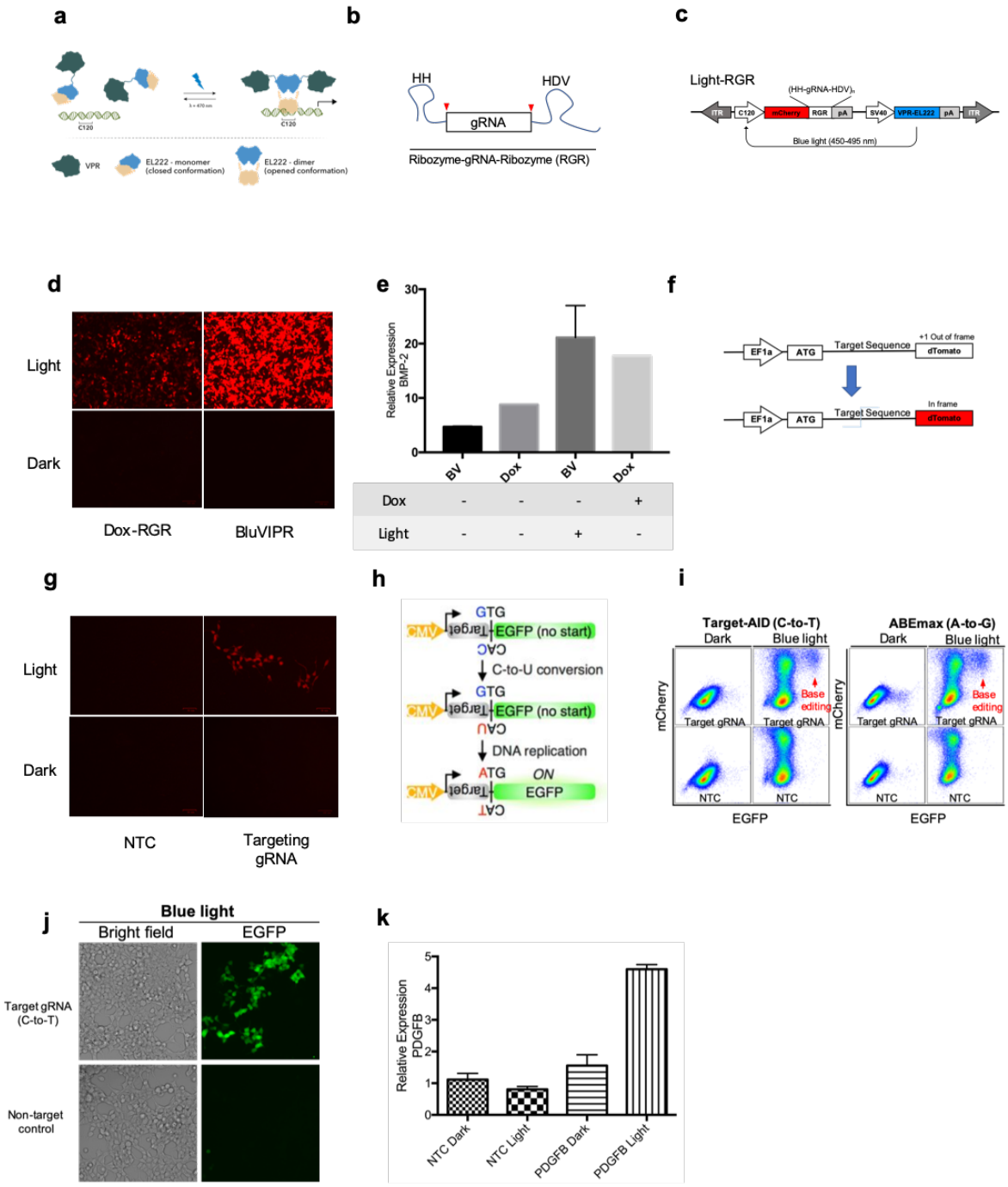

Figure 3: BluVIPR as an orthogonal optogenetic CRISPR/Cas system: a. Schematic overview of VPR-EL222 function, b. Schematic of RGR, c. Schematic of BluVIPR plasmid, d. BluVIPR compared to Tet-On activation of mCherry (1mW/cm2 470nm activation, 24 hours), e. BluVIPR compared to Tet-On CRISPRa activation of BMP-2 (1mW/cm2 470nm activation, 24 hours, n=3), f. Schematic of dTomato reporter for Cas9 nuclease function, g. BluVIPR activation of Cas9 nuclease reporter cells, top right panel shows edited cells; NTC: Non-target Control(1mW/cm2 470nm activation, 24 hours, imaged 48 hours post stimulation), h. Schematic of C-to-T Base Editing reporter, i. BluVIPR activation of C-to-T and A-to-G base editors (1mW/cm2 470nm activation, 24 hours) top panels show mCherry expressing cells and a distinct double positive population of edited cells, j. BluVIPR activation of C-to-T base editor (1mW/cm2 470nm activation, 24 hours, cells imaged 48 hours post stimulation), k. BluVIPR activation of dCas12a-VPR results in 4-fold activation of PDGFB upon light stimulation (1mW/cm2 470nm activation, 48 hours).

The versatility of light-induced gRNA expression also allows for spatiotemporal control of orthologous Cas proteins *in vivo*. To demonstrate this, we used zebrafish embryos (3 days post fertilization) to demonstrate spatiotemporal control of precise base editing *in vivo*. HEK293T C-to-T base editing reporter cells were transfected with Target-Aid and BluVIPR expressing a gRNA designed to activate C-to-T base editing, and subsequently injected into the zebrafish yolk sack (Figure 4a). By illuminating a spatially defined region of the zebrafish embryo, we could activate the base editor reporter (EGFP), confirmed by light-sheet microscopy (Figure 4b). To demonstrate the compatibility of BluVIPR with commercially available CRISPR/Cas mouse models, we used neural stem cells (NSCs) from Cas9 mice (Gt(ROSA)26Sor$^{tm1.1(CAG-cas9*,-EGFP)Fezh}$) to optogenetically target EGFP (Figure 4c). The NSCs from these mice constitutively express SpCas9 and EGFP. We transfected murine NSCs with BluVIPR containing an EGFP-targeting RGR and upon exposure to blue light, Blue-light induced activation of mCherry reporter was evidenced (Figure 4d).

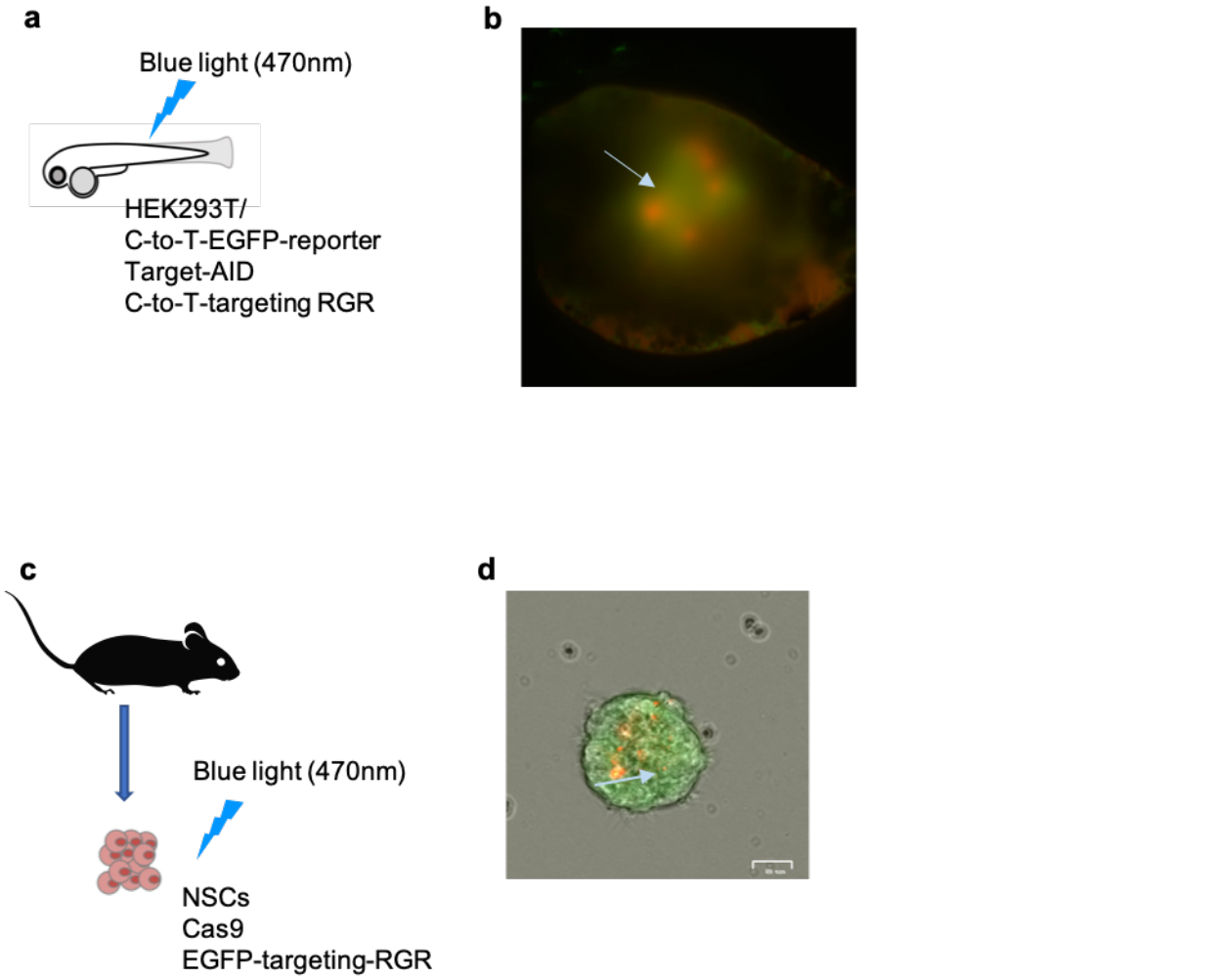

Figure 4 BluVIPR is active in vivo: a. Schematic of zebrafish experiment, C-to-T reporter cells were injected into yolk sack and stimulated with Light Sheet microscope (2 minute activation, continual scanning of yolk sack with 488nm laser, followed by 10 minutes of darkness, repeated for 5 cycles), embryos were imaged with light sheet microscope 24 hours post stimulation, b. C-to-T reporter cells exhibit mCherry and EGFP, indicating both BluVIPR activation of mCherry and base editor activity, c. Schematic of Mouse NSC experiment, NSCs were isolated from Cas9 mice, transfected, and stimulated (1mW/cm2 470nm activation, 24 hours) then imaged 24hours post stimulation.

In summary, the overall data presented indicates an efficient system for optogenetic control of gRNA expression, allowing for complete spatiotemporal control, multiplexing and fully orthogonal CRISPR/Cas regulation. This system can be used to optogenetically activate different SPCas9 variants and even other species and type of Cas. The ability to harness the full spectrum of CRISPR/Cas tools with an optogenetic means of control opens up many exciting avenues of research and has potential therapeutic implications. Such a system has uses in virtually any imaginable genome, epigenome, or transcriptome engineering application where precise spatiotemporal regulation is desired.

ADDITIONAL INFORMATION

METHODS

Cell culture

HEK293T (Espinosa laboratory stock) were cultured in high-glucose DMEM (Sigma Aldrich) supplemented with fetal calf serum (10%), streptomycin (0.1 mg/ml), penicillin (100 U/ml), Sodium pyruvate (1 mM) (Sigma Aldrich), HEPES (10 mM) (Sigma Aldrich) and L-glutamine (2 mM) (Sigma Aldrich). Cells were routinely tested for mycoplasma contamination. Transfections of HEK293T cells were performed using X-tremeGENE 9 DNA Transfection Reagent (Roche). All experiments/transfections were performed in triplicate.

Plasmid constructs

pRS0045 (Addgene #131124)

pRS0035 (Addgene #131125)

lentiCRISPR v2 (Addgene #52961)

pLV-SI-121 (Addgene #131126)

pLV-SI-112 (Addgene #131127)

pCMV_ABEmax (Addgene #112095)

pXR001 (Addgene #109049)

pSBtet-GB (Addgene #60504)

gRNA-Cloning (Addgene #41824)

SP-dCas9-VPR (Addgene #63798)

CRISPR-SP-Cas9 reporter (Addgene #62733)

BluVIPR plasmids will be deposited to Addgene.

Gene fragments were synthesized (GeneStrands, Eurofins; gBlocks, IDT). Gene synthesis was performed by Eurofins. Some fragments from existing constructs were replicated with PCR using Platinum Pfx DNA polymerase (ThermoFisher). Constructs were assembled by Gibson assembly (Gibson Assembly® Master Mix (New England Biolabs)) and golden gate assembly. All assembled constructs were verified by Sanger sequencing and restriction digests.

Table 1 gRNA sequences

gRNA Target	Sequence
dTomato Reporter	GGGCCACTAGGGACAGGAT
Cas 9 NTC	GAACGACTAGTTAGGCGTGTA
BMP-2	GGCGAGCCGCGCCGCGAAGG
C-to-T reporter	CACGGTCACCCTGACACGCT
A-to-G reporter	CCTTATGACCCTGACACGCT
Cas12a PDGFB	TAAAGGAGAAGGGAGAGTGCGAG
Cas12a NTC	GAACGACTAGTTAGGCGTGTA

Optogenetic experiments

BluVIPR activity assay

HEK293T cells were seeded in black walled, optical bottom 96 well plates (Thermo Scientific, 165305) at 40,000 cells/well. Cells were transfected with BluVIPR plasmid (50ng) immediately after seeding. 24 hours after transfection, cells were stimulated with 1mW/cm^2 of 470nm light on a custom made transilluminator. Fluorescence micrographs were taken on a Zoe fluorescent cell imager (Bio-rad) after 24 hours of stimulation.

BluVIPR CRISPRa assay

HEK293T cells were seeded as described for BluVIPR activity assays and transfected with SP-dCas9-VPR and BluVIPR plasmids with targeting and non-targeting gRNA RGRs (all

gRNA sequences are described in table 1) (50ng of each). Cells were stimulated after 24 hours with 1mW/cm^2 of 470nm light and harvested 24 hours later for RNA extraction and qPCR.

SPCas9 and Base Editor Reporter cell line generation

HEK293T cells were seeded in 6 well plates (2x10^5 cells/well) and transduced with 25µl of lentiviral vectors (CRISPR-SP-Cas9 reporter, pLV-SI-121, or pLV-SI-112). Puromycin selection (2.5µg/ml) was started 48 hours post-transduction. Surviving colonies were kept under selection pressure and used for further experiments after 7 days.

SPCas9 reporter assay

SPCas9 reporter cells were seeded as described for BluVIPR activity assays and transfected with lentiCRISPR v2 and BluVIPR plasmids with targeting and non-targeting gRNA RGRs (50ng of each). Cells were stimulated after 24 hours with 1mW/cm^2 of 470nm light. Fluorescence micrographs were taken on a Zoe fluorescent cell imager (Bio-rad) after 48 hours of stimulation.

Base Editor Assays

Base editor reporter cells were seeded as described for BluVIPR activity assays and transfected with pCMV_ABEmax/ pRS0035 and BluVIPR plasmids with targeting and non-targeting gRNA RGRs (50 ng of each). Cells were stimulated after 24 hours with 1mW/cm^2 of 470nm light. Cells were harvested for flow cytometry 24 hours later (Gallios Flow cytometer, Beckman Coulter), or kept in the dark after stimulation and fluorescence micrographs were taken on a Zoe fluorescent cell imager (Bio-rad) after 48 hours.

BluVIPR CRISPRs Cas12a-VPR

HEK293T cells were seeded as described for BluVIPR activity assays and transfected with LB dCas12a-VPR (3ng), BluVIPR plasmids with targeting and non-targeting gRNA RGRs (70ng of each). Cells were stimulated after 24 hours with 1mW/cm^2 of 470nm light, and harvested 48 hours later for RNA extraction and qPCR.

Zebrafish imaging

Base editor reporter cells were seeded in T75 flasks (2x10^{6}cells per flask) and allowed to grow to 70-80% confluence. Cells were transfected with pRS0035 and BluVIPR vector with targeting gRNA (5 µg each) and kept in the dark overnight. Cells were harvested and resuspended in 2% w/v Polyvinylpyrrolidone (Sigma) in PBS. Cells were injected into the yolk sack of 3 days post fertilization zebrafish embryos (n=3). After 12 hours, embryos were stimulated with a Carl Zeiss Z.1 lightsheet microscope (2 minute activation, continual scanning of yolk sack with 488nm laser, followed by 10 minutes of darkness, repeated for 5 cycles), then kept in the dark. Embryos were imaged 24 hours after stimulation with the same microscope.

Mouse NSCs

The subventricular zone (SVZ)-derived neural progenitor cells (NPCs) were isolated according to a modified protocol by **Johansson et al. (1999)**[108,109]. Briefly, SVZ biopsies were isolated and the cells dissociated. For isolation of the NPCs, mechanical and enzymatic dissociation using 200 U/ml DNase (Sigma-Aldrich) and 10 U/ml papain (Worthington) was used. The cells were washed in 0.9 M sucrose in Hanks balanced salt solution (Invitrogen) to

remove the myelin debris. The cells were cultured in propagation medium, composed of DMEM/F-12 containing B27 supplement (Invitrogen), penicillin (100 U/ml), and streptomycin (100 μg/ml) (Invitrogen), 20 ng/ml epidermal growth factor (EGF, Sigma-Aldrich), and 20 ng/ml basic fibroblast growth factor (bFGF, R&D systems).

Cells were electroporated with BluVIPR with gRNA targeting EGFP. Cells were stimulated after 24 hours with 1mW/cm^2 of 470nm light. Fluorescence micrographs were taken on a Zoe fluorescent cell imager (Bio-rad) and subsequently cells were harvested for flow cytometry 24 hours later (Gallios Flow cytometer, Beckman Coulter).

Luciferase assays

We used X-tremeGENE 9 (Roche) to transfect HEK293T cells in 96-well plates (40,000 cells/well, 50ng per construct). pRL-CMV-Renilla (5ng) for normalization. Luminescence was measured 24 hours post-transfection using the Modulus Single Tube Reader (Promega). Relative luminescence (RLU) is reported as firefly (Photinus) luciferase signal divided by Renilla luciferase signal.

Quantitative PCR

All RNA extractions were performed using TRIzol (Invitrogen). cDNA conversions were performed using the High Capacity cDNA Reverse Transcription Kit (Applied Biosystems) or the iScript cDNA Synthesis Kit (Bio-Rad). Gene expression was determined using TaqMan gene expression assays (Thermo Fisher Scientific): PDGFB (Hs00966522_m1), HPRT1 (Hs01003267_m1), BMP2 (Hs00154192_m1). The reactions were performed using the Light Cycler 96 real-time PCR system (Roche), and data were analyzed using the Light Cycler 1.1 software (Roche).

Statistical analysis

Statistical analyses were performed using R (R 3.4.4) or Prism 6 (GraphPad Software). One-way ANOVA and post-hoc Tukey tests were performed to assess significance, with $p<0.05$.

SUPPLEMENTARY

EL222 activation

HEK293T cells were seeded in black walled, optical bottom 96 well plates (Thermo Scientific, 165305) at 40,000 cells/well. Cells were transfected with EL222-Luc (50ng) and pRL-CMV-Renilla (5ng) for normalization. Luminescence was measured 24 hours post-transfection using the Modulus Single Tube Reader (Promega). Relative luminescence (RLU) is reported as firefly (Photinus) luciferase signal divided by Renilla luciferase signal. Modest activation of Luciferase was evidenced after blue light stimulation (fig 3).

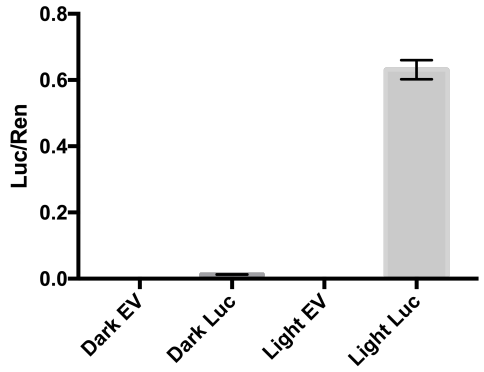

Figure 5 VP16-EL222 activation of Luciferase reporter. EV: Empty vector control.

BluVIPR vs VP16-EL222

HEK293T cells were seeded in black walled, optical bottom 96 well plates (Thermo Scientific, 165305) at 40,000 cells/well. Cells were transfected with BluVIPR or EL222-mCherry plasmid (50ng) immediately after seeding. 24 hours after transfection, cells were stimulated with 1mW/cm^2 of 470nm light on a custom made transilluminator. Fluorescence micrographs were taken on a Zoe fluorescent cell imager (Bio-rad) after 24 hours of stimulation. Robust expression of mCherry was evidenced in the BluVIPR groups (Figure 6).

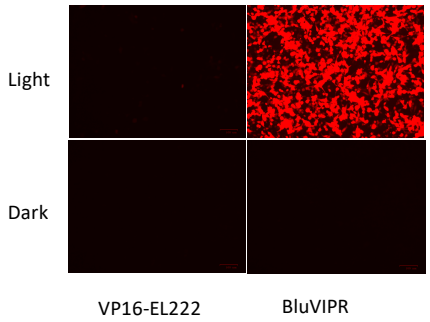

Figure 6 BluVIPR vs VP16-EL222

CHAPTER 4

AIR GAP ELECTROSPUN TEMPLATES WITH BLUE LIGHT GRADIENT FOR ENGINEERED CELL STIMULATION

INTRODUCTION

Anterior cruciate ligament reconstruction surgery has high repair failure, mostly due to the current inability to regenerate a properly functioning enthesis[93]. The specialized interface referred to as the enthesis, the insertion of tendons/ligaments into bone, is a highly-organized tissue presenting continuous gradients of structural and mechanical properties that allow smooth force transfer, protecting and maintaining the tendon/ligament insertion. The mechanical properties of the enthesis arise from a gradient of cell type/morphology, extracellular matrix (ECM), and minerals that transition smoothly from tendon/ligament to bone (Figure 7). The lack of regeneration of the enthesis leads to high failure rates after these procedures due to formation of a discrete transition of tissue characteristics which acts as a force concentrator that, under mechanical loading, is the site of rupture. The structural and mechanical gradients of entheses are critical for normal function and regenerating these gradients is a major challenge. Here we present a possible strategy for utilization of an air gap electrospun template delivering a blue light gradient to engineered cells to promote growth factor production as an interfacial tissue engineering approach.

The development of the enthesis occurs postnatally, although the exact process is poorly understood. A combination of physicochemical stimuli drive the gradient formation in the interfacial structure. Transcription factors Sox9 and Scleraxis (Scx) play important roles in the development of the enthesis, and are arranged in opposing gradient fashion in immature postnatal entheses (Figure 7). Previous studies have reported that arranging growth factors on porous

membranes in opposed gradients leads to differentiation of progenitor cell populations and arrangement of structural properties reminiscent of a native enthesis[97].

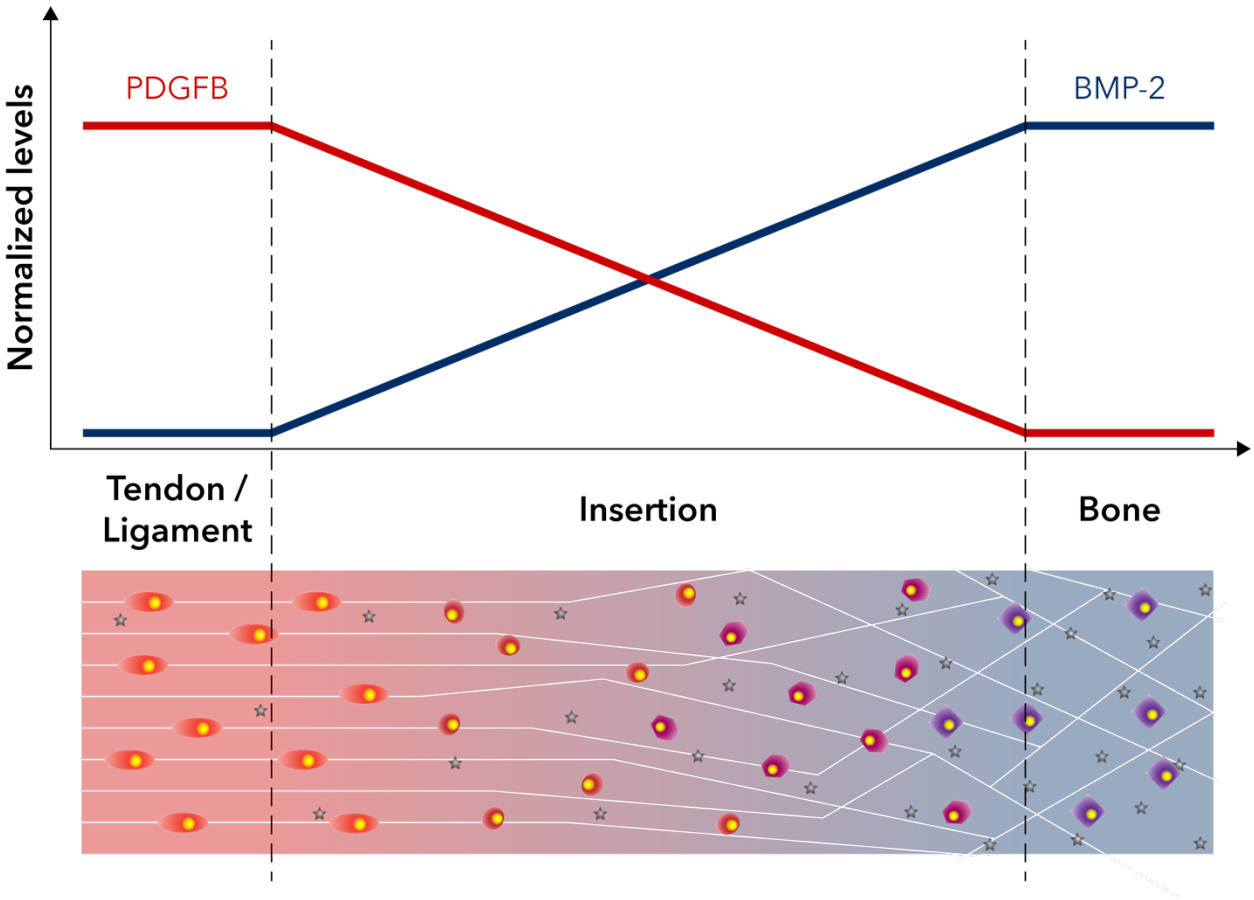

Figure 7 Schematic of enthesis structural gradient and growth factor opposed gradients that give rise to the entheseal tissue characteristics.

Electrospinning is a popular process for nanofiber production, leading to porous membranes, involving a charged polymer solution jet collected on a grounded target[110]. Typically, electrospun templates are randomly deposited, non-woven fibers, but several approaches can be used to generate spatially organized fibers[110,111]. Air gap electrospinning uses equidistant grounded targets separated in space to collect fibers, resulting in aligned structures that mimic the native ligament[111,112]. Air gap electrospinning is thus a viable technique to

produce templates with highly aligned fibers that promote appropriate cellular morphology, function, organization, and infiltration[111]. Electrospun templates made of polycaprolactone (PCL) are widely used in tissue engineering, and their degradation and biocompatibility characteristics are well known[111]. Furthermore, aligned nanofiber templates have been shown to promote tendon-like tissue formation, which would be exploited for development of the tendon proper along the template, changing in a gradual fashion towards a bone tissue when approaching a light source[93,97,111].

For the development of the delivery of gradient stimuli, we chose blue light, expecting diffusion through the template according to Beer-Lambert's Law. The hypothesis is that by illuminating an aligned-fiber electrospun scaffold on one end, the light will generate a gradient in the template longitudinal axis. The light dose is thus titrated in a smooth gradient and can be used to stimulate cells to produce growth factors following this gradient. A wide variety of optogenetic tools are being developed and could be used to engineer the cells to be used with these templates[75,76,90,92]. In this initial study, we present the development of air gap electrospun PCL templates that emulate tendon or ligament morphology and mechanical properties. Furthermore, we describe the generation of a blue light gradient in a physiologically-relevant scale for enthesis regeneration, through the potential stimulation of engineered cells that would deposit growth factors in gradient fashion, mimicking entheseal development.

MATERIALS AND METHODS

ELECTROSPINNING

Polycaprolactone (MW 80,000; 440744; Sigma) was dissolved overnight in 1,1,1,3,3,3 hexafluoro-2-propanol (HFP, Oakwood Products) at 100 mg/ml concentration. Electrospinning parameters were +25KV, 10 cm distance from needle to collection targets, 5 cm air gap between

collection targets, 3 ml/hr flow rate through an 18 gauge blunt needle, and collected on a rotating air gap mandrel. Airgap electrospinning apparatus was based on the system described by Sell et al., and was 3D printed in-house from polylactic acid filament[111]. Templates were allowed to dry in desiccator at room temperature for at least 24 hours before any subsequent experiments.

NANOFIBER MEASUREMENT

Templates were imaged using scanning electron microscopy (SEM, FEI NN650 FEG, Noca NanoSEM with field emission gun) at +20kV, working distance of 5mm, and 1,000X magnification, and fiber diameter was measured with FibraQuant 1.3 software (NanoScaffold Technologies) (n=3). Average fiber diameter was calculated using 300 random measurements per template. Computer-generated measurements were checked visually to ensure accurate diameter of fibers were measured, and that few or no repeated measurements were analyzed.

MECHANICAL TESTING

Uniaxial tensile testing was performed on dog-bone shaped samples (2.75mm at narrowest width, 7.5mm gauge length), using a TestResources frame (model: 220Q). Samples (n=5) were allowed to proceed to failure at a strain rate of 10mm/min. Force -Elongation curves were recorded with XY software (TestResources).

BLUE LIGHT GRADIENT CHARACTERIZATION

To analyze the gradient in blue light intensity along the longitudinal axes of the templates, samples (n=5) were illuminated from one end with an OpalDrive laser source (470nm wavelength; 20mW, Ellumiglow) and Laser Wire guide (Ellumiglow) and images acquired with a Pariss Imaging Microscope (LightForm). A path was drawn from the edge of the sample, and the intensity of each pixel along this path was calculated with ImageJ software, and plotted along the longitudinal axis.

RESULTS

Templates had an average fiber diameter of 519±120nm. Fibers were aligned and presented similar morphology to ligament ECM (Figure 8)[113]. Noteworthy are the undulating fibers, similar to the crimped (relaxed) structure in native tendon/ligament collagen fibrils. It is likely that the mechanical shock absorber function these undulating structures play in native tissues would be replicated by to the air gap electrospun templates. To test this, we performed mechanical testing on the templates.

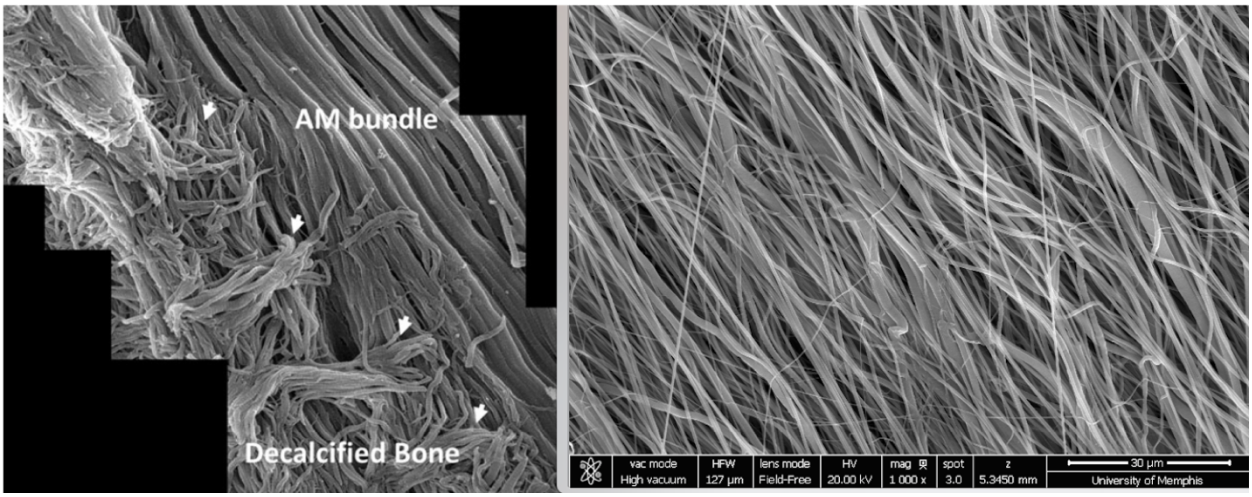

Figure 8: Representative SEM micrograph of air gap electrospun PCL templates compared to native pig ACL enthesis. On the left is a pig ACL enthesis (l. Zhao, et al.), on the right is a representative image of our templates.

Uniaxial tensile testing showed that templates exhibit similar characteristics to natural pig ligament, albeit with less ultimate stress at failure[114]. Particularly interesting is the presence of an initial concave area, a linear range, and initial failure point in the stress-elongation curves (Figure 9). The ultimate stress at failure was 28000±2500 KPa.

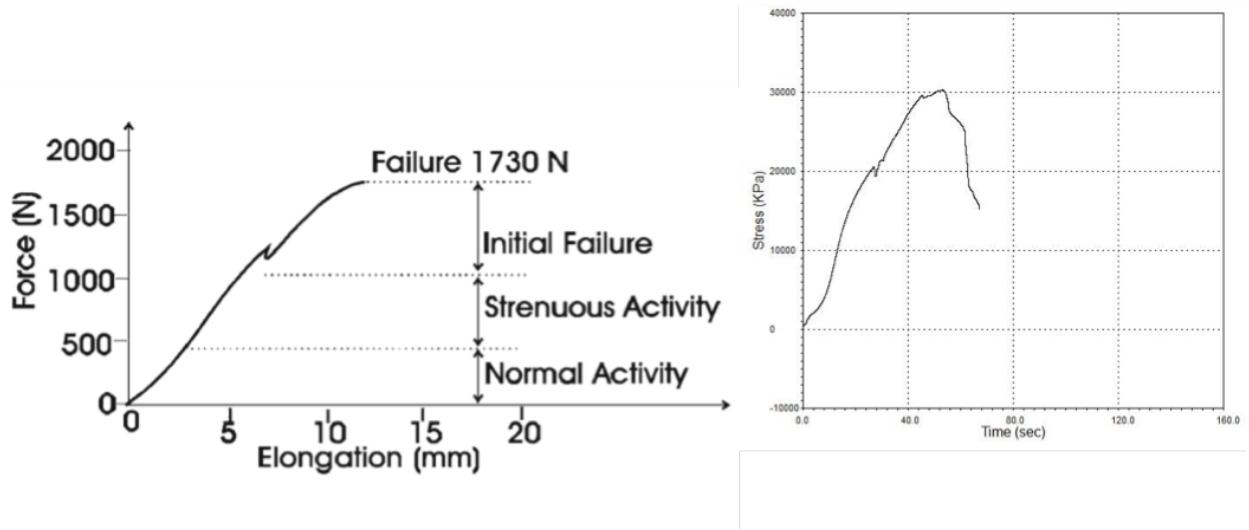

Figure 9: Representative Stress-Elongation curve for air gap electrospun templates compared to native ligaments. On the left is a force-elongation curve from tensile strength test on pig ligaments (S. Pal et al., 2014). On the right is a representative curve from our templates.

Templates were illuminated with the OpalDrive laser source and Laser Wire guide in direct contact and perpendicular to the longitudinal axis of the template. The laser wire is 900µm in diameter and was affixed directly adjacent to the template on a clear cover slip. The single power setting on the laser source module consistently casted light through the fibers, and a light gradient was readily apparent under microscopic observation. Blue light gradients were exhibited on the first 400±100µm of the template, and correspond to the desired range of enthesis depth - 200-500µm (Figure 10).

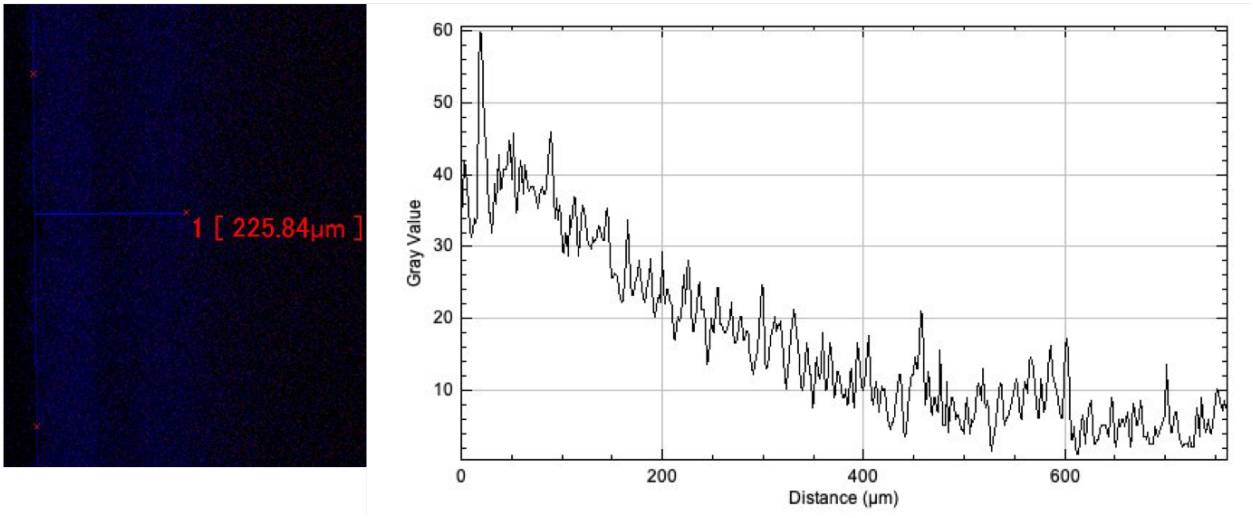

Figure 10: Representative pixel intensity plot along template longitudinal axis. On the left is a representative micrograph of the blue light gradient on our templates. Point 1 (225um) is estimated 50% intensity point as measured by the Pariss Imaging Microscope.

DISCUSSION

The fibers generated with the air gap electrospinning setup were of appropriate diameter, aligned and showed undulating patterns that closely resemble native tissue ECM. The similarity to the natural substrate should allow engineered cells to attach and flourish on and in the templates. Ultimate stress at failure was significantly lower for the templates than what is reported in literature for native ACL (35 MPa)[115]. This could be explained by the thickness of the tested samples (average of 0.05mm). Thicker templates could likely increase the ultimate stress at failure. Regardless, the shape of the stress-elongation curves show similar important structural properties to native ACL.

The blue light gradients exhibited on the templates behaved as expected for the presentation of cues to engineered cells in ACL regeneration strategies that we propose. The intensity of light, and subsequent gradient generation and depths, could be tailored with the use of a variable power output laser source. Light gradient properties could also be modulated through material composition and fiber characteristics through electrospinning parameter manipulation. Altogether, the data presented shows that air gap electrospun templates have

biomimetic characteristics (morphological and mechanical) and are amenable to the generation of a blue light gradient for optogenetic stimulation of growth factor production by engineered cells. This combination should be useful in the directed differentiation of cells to populate the enthesis. This study is the first to elucidate the possibility of presenting engineered cells with blue light stimulation in a gradient fashion for interfacial tissue engineering, and is a proof of concept of how the templates could deliver these stimuli.

CONCLUSION

Biomaterial-mediated optogenetics could provide an alternative approach to spatiotemporal patterning of growth factors for tissue engineering, and would be of special interest to interfacial tissue regeneration, as recapitulating the gradient nature of interfaces is a challenging goal for regenerative medicine. This work presents a proof of concept for how electrospun templates could be used as vehicles for gradient stimulation of engineered cells with blue light. This is a first step towards characterizing how light interacts with electrospun fibers, providing a springboard for future development of integrated systems with engineered cells.

CHAPTER 5

CRISPR/CAS-BASED DIGITAL DEMULTIPLEXER CIRCUIT TO GENERATE COUNTER-OPPOSED GRADIENTS OF GROWTH FACTORS FOR INTERFACIAL TISSUE ENGINEERING

INTRODUCTION

The enthesis, as an example of an interfacial tissue, arises in embryonic development through the generation of counter-opposed gradients of growth factors that direct an arrangement of cells, signals, and extracellular matrix[93,94]. The specialized interface referred to as the enthesis, the insertion of tendons/ligaments into bone, is a highly-organized tissue presenting continuous gradients of structural and mechanical properties that allow smooth force transfer, protecting and maintaining the tendon/ligament insertion[93,94,96]. The lack of regeneration of the enthesis leads to high repair failure rates, due to formation of a discrete transition of tissue characteristics which acts as a force concentrator that, under mechanical loading, is the site of rupture[93]. Tissue engineering approaches that mimic the developmental process of polarization of a pool of progenitor cells through growth factor counter-gradients could be a promising approach to regenerate entheseal structures. Though the presentation of signals in appropriate spatiotemporal patterns is a fundamental concept of tissue engineering, current strategies rely heavily on the use of recombinant proteins and fabrication strategies to present these proteins to cells[100,116,117]. These recombinant proteins must often be delivered in supraphysiological doses that increase cost and potential side effects[116–118]. A solution that utilizes simple, genetically-encoded, synthetic gene regulatory networks could provide an elegant means of directing cell production of endogenous growth factors with easily controlled and cost-effective physico-chemical stimuli.

In this chapter, we discuss the concept and preliminary work towards building such a solution: a chemo-optogenetic, CRISPR/Cas-based digital demultiplexer circuit.

CRISPR/Cas systems are RNA-guided restriction machineries that evolved as primitive acquired immune systems in prokaryotes[62,102]. Bacteria and archaea utilize this machinery to defend themselves against mobile genetic elements, such as phages. In this evolutionary arms race, phages have responded by evolving small proteins that hinder CRISPR/Cas mechanisms: Anti-CRISPR proteins (Acr)[119,120]. These Acr are highly specific, and show great affinity for their targets. Both CRISPR and Anti-CRISPR elements have been utilized to develop tools for genome engineering, and form the basis for the demultiplexer circuit described here[121].

A demultiplexer is a circuit that uses a data input and one, or multiple, selection inputs to assign values to outputs depending on the selection inputs[122]. If the data input is constant, the selection input can influence the outputs in opposite functions (like an OR gate), allowing the demultiplexer to act as a binary decoder[122]. This effectively converts a serial signal into a parallel output, allowing for one stimulus to have multiple effects, depending on design. The demultiplexer described in this chapter uses doxycycline (or transcription from constitutive promoters) as a constant data input, and blue-light (470nm) as a selection input. BluVIPR, as an optogenetic control system allowing for transcription of both protein-encoding sequences and gRNA, is the tool that allows to switch the selection input into a binary code. The BluVIPR-mediated, light-induced production of gRNA specifically targets one growth factor transcriptional regulation sequence for activation (BMP-2) via SPdCas9, while upstream of the RGR, an Acr-encoding sequence (AcrVa1) specifically targets LBdCas12a. In the complete circuit, detailed in Figure 11, LBdCas12a-VPR is targeted to activate transcription of another growth factor (PDGFB). This logic allows blue light to activate transcription and production of

BMP-2, and simultaneously inhibit the CRISPRa activation of PDGFB. Based on data that suggests that counter-opposed gradients of bone morphogenetic protein 2 (BMP-2) and platelet derived growth factor B (PDGFB) can drive differentiation recapitulating the cellular and extracellular matrix distribution of entheses, we chose to use these growth factors as targets for the outputs of the circuit[97]. Utilizing this demultiplexer, cells that have been programmed will respond to a gradient of blue light by producing counter-opposed gradients of BMP-2 and PDGFB, driving polarization and mimicking the developmental conditions that give rise to entheseal structures.

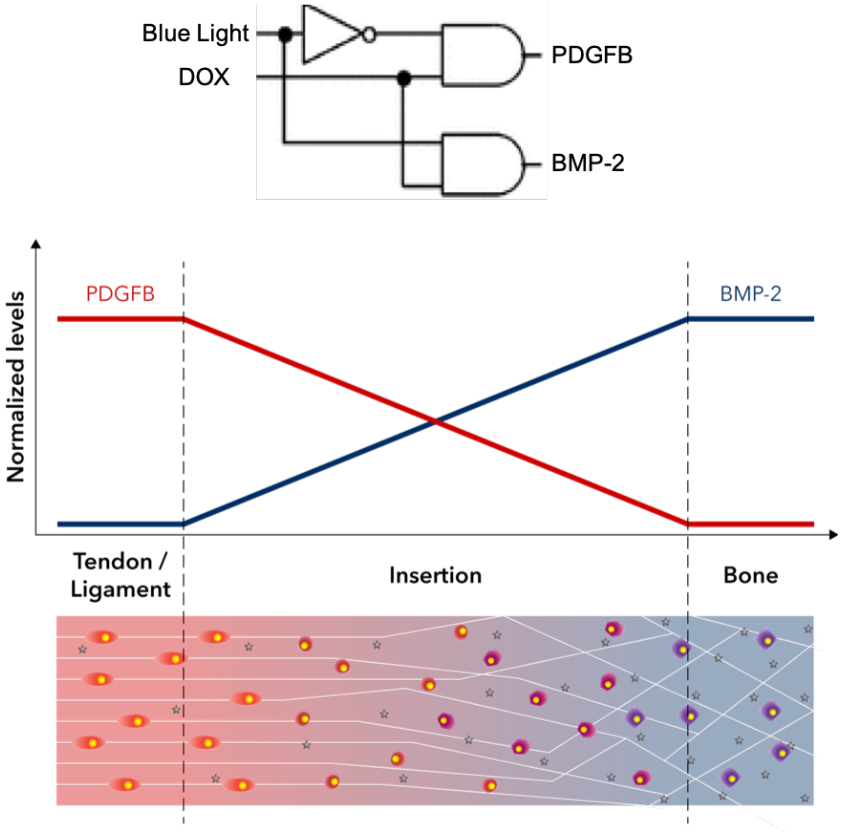

Figure 11 Schematic of BluVIPR digital demultiplexer circuit and the growth factor opposing gradients formed in response to a blue light gradient.

MATERIALS AND METHODS

Cell culture

HEK293T (Espinosa laboratory stock) were cultured in high-glucose Tet-approved DMEM (Sigma Aldrich) supplemented with fetal calf serum (10%), streptomycin (0.1 mg/ml), penicillin (100 U/ml), Sodium pyruvate (1 mM) (Sigma Aldrich), HEPES (10 mM) (Sigma Aldrich) and L-glutamine (2 mM) (Sigma Aldrich). Cells were routinely tested for mycoplasma contamination. Transfections of HEK293T cells were performed using X-tremeGENE 9 DNA Transfection Reagent (Roche). All experiments/transfections were performed in triplicate.

Plasmid constructs

Lenti-EF1a-dCas9-VPR-Puro (Addgene #99373)

SP-dCas9-VPR (Addgene #63798)

PB-TRE-dCas9-VPR (Addgene #63800)

pRL-CMV-Renilla (Promega)

BMP-2 Luciferase reporter (SwitchGear Genomics)

gRNA cloning vector (Addgene #41824)

BluVIPR and demultiplexer plasmids will be deposited to Addgene.

Gene fragments were synthesized (GeneStrands, Eurofins; gBlocks, IDT). Gene synthesis was performed by Eurofins. Some fragments from existing constructs were replicated with PCR using Platinum Pfx DNA polymerase (ThermoFisher). Constructs were assembled by Gibson assembly (Gibson Assembly® Master Mix (New England Biolabs)) and Golden Gate assembly. All assembled constructs were verified by Sanger sequencing and restriction digests.

gRNA screens

The sequences used for all the gRNA screens were designed with the Genetic Perturbation Platform's sgRNA Designer webtool (Broad Institute). Sequences were chosen to target 75 to 300 base pairs upstream of the target gene's TSS, using the Human GRCh38 reference genome, and respective Cas to be used (SPCas9 (NGG PAM) or LBCas12 (TTTV PAM)).

We used X-tremeGENE 9 (Roche) to transfect HEK293T cells in 96-well plates (40,000 cells/well) SP-dCas9-VPR (50ng), gRNA cloning vector (50ng) (all gRNA sequences are described in table 1), BMP-2 luciferase reporter (50ng), and pRL-CMV-Renilla (5ng) for normalization. Luminescence was measured 24 hours post-transfection using the Modulus Single Tube Reader (Promega). Relative luminescence (RLU) is reported as firefly (Photinus) luciferase signal divided by Renilla luciferase signal.

Optogenetic experiments

BMP-2 AND gate

HEK293T cells were seeded in black walled, optical bottom 96 well plates (Thermo Scientific, 165305) at 40,000 cells/well and transfected with PB-TRE-dCas9-VPR and BluVIPR plasmids with targeting and non-targeting gRNA RGRs (50ng of each). Cells were stimulated after 24 hours with 1mW/cm^2 of 470nm light on a custom made transilluminator and Doxycycline (2. 5µg/ml), in combinations according to AND gate logic (-/-, +/-, -/+, +/+) and harvested 24 hours later for RNA extraction and qPCR.

Promoter Comparison for SPdCas9VPR

HEK293T cells were seeded as described for BMP-2 AND gate experiments and transfected with SP-dCas9-VPR/lenti-EF1a-dCas9-VPR-Puro and BluVIPR plasmids with

targeting and non-targeting gRNA RGRs (50ng of each). Cells were stimulated after 24 hours with 1mW/cm^2 of 470nm light and harvested 24 hours later for RNA extraction and qPCR.

RESULTS

BMP-2 CRISPRa gRNA screen

Ten different SPCas9 gRNA sequences targeting upstream of the TSS of BMP-2 were screened to evaluate activation of transcription via SPdCas9-VPR. While most of the gRNAs exhibited strong activation of the luciferase reporter, three gRNA sequences failed to induce any significant activation (Figure 12). Sequence number two (GGCGAGCCGCGCCGCGAAGG) showed the highest activation, and was chosen for subsequent experiments.

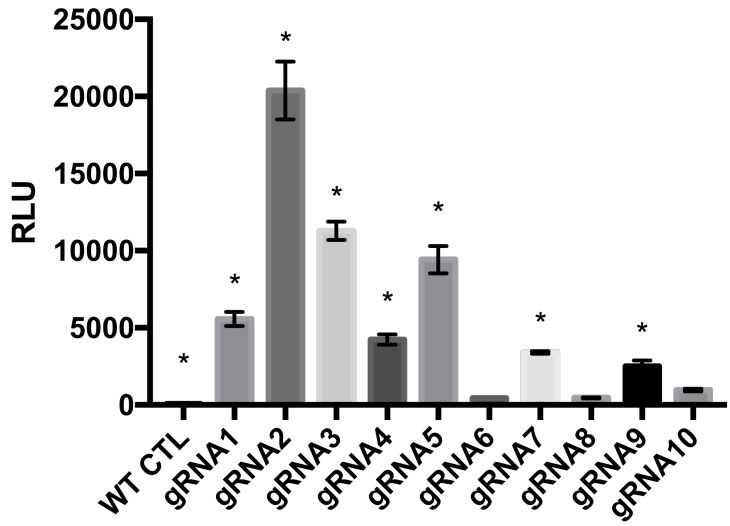

Figure 12 gRNA sequence screen for SPdCas9-VPR activation of BMP-2

BMP-2 AND gate

A chemo-optogenetic AND gate, responding to blue light and doxycycline, was generated to drive BMP-2 transcription activation (Figure 13). Two plasmids were used, a Tet-On plasmid driving SPdCas9-VPR under doxycycline control, and a BluVIPR plasmid driving gRNA production under blue light control. Cells that were exposed to both blue light and

doxycycline exhibited strong activation of BMP-2 (Figure 13). Cells that were in the dark, or only exposed to doxycycline, exhibited low levels of background BMP-2 production. Notably, cells that were only exposed to blue light exhibited a high production of BMP-2, suggesting that the leakiness of the Tet-On promoter was allowing for a significant level of SPdCas9VPR to be present in basal conditions, without doxycycline stimulus.

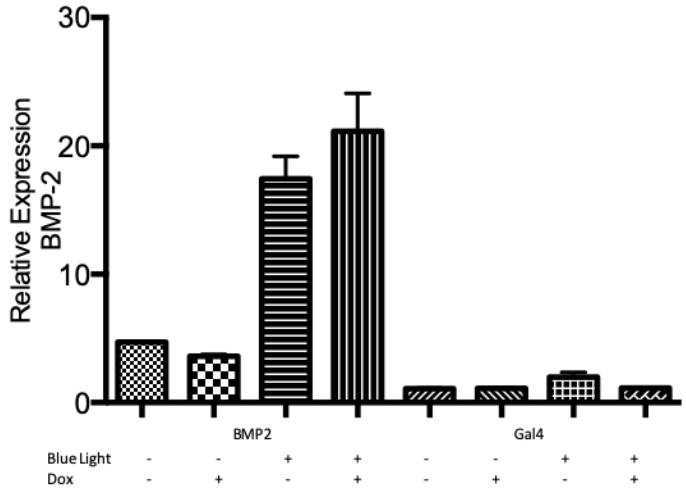

Figure 13 Blue Light and Doxycycline responsive AND gate for BMP-2 production

Promoter comparison for SPdCas9-VPR

To investigate if lower basal levels of SPdCas9-VPR would lead to lower background levels, a comparison of CMV and EF1a promoters was performed. When combined with light-inducible gRNA, EF1a exhibited a lower activation, a conserved dynamic range, and a lower background BMP-2 level (Figure 14). These data suggest that lower SPdCas9-VPR levels indeed lead to lower background levels.

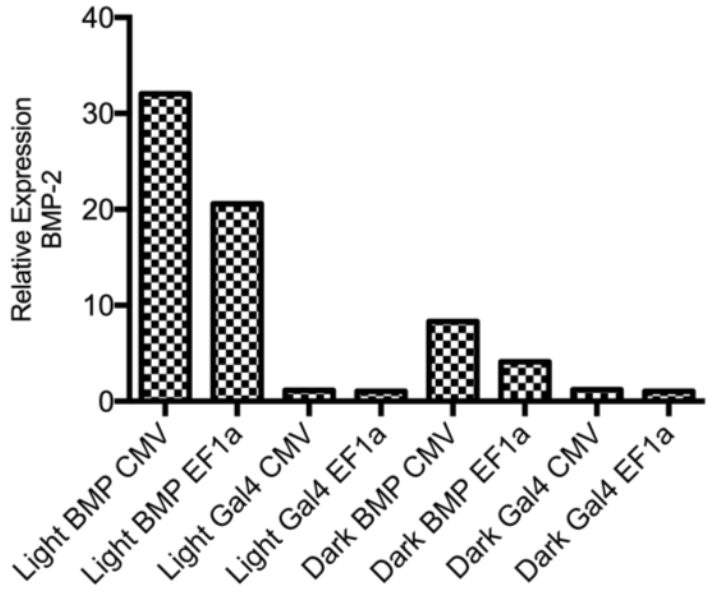

Figure 14: CMV vs EF1a promoters for Cas9 transcription and BluVIPR activation of BMP-2.

PDGFB gRNA Screen

Eight different LBCas12a gRNA sequences targeting upstream of the TSS of PDGFB were screened to evaluate activation of transcription via LBdCas12a-VPR. While four of the gRNAs exhibited strong activation of the target gene, four gRNA sequences failed to induce any significant activation (Figure 15).

Sequence number seven (TAAAGGAGAAGGGAGAGTGCGAG)

showed the highest activation, and was chosen for subsequent experiments.

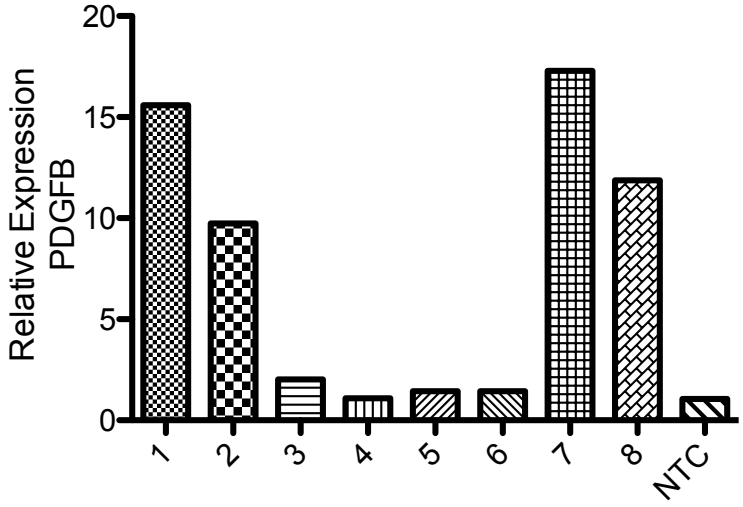

Figure 15:gRNA screen for LBCas12a-VPR activation of PDGFB.

DISCUSSION AND CONCLUSION

In this chapter we have presented the concept and preliminary work towards a simple, genetically-encoded, chemo-optogenetic demultiplexer circuit to direct cells to produce counter-gradients of growth factors upon physico-chemical stimulation. In the previous chapter, we discussed the delivery of a blue light gradient using electrospun templates. Together, these two chapters present the tools that allow the possibility of biomaterial-mediated optogenetic stimulation for counter-gradient growth factor production and polarization of cell populations.

The gRNA screens for SPdCas9-VPR activation of BMP-2 and LBdCas12a-VPR activation of PDGFB showed that, while most gRNAs designed and tested showed activation of target genes, some were clearly more active than others. It is thus important to perform these screens for each target gene when designing these circuits.

The demultiplexer circuit can be envisioned as two AND gates that have a constant input and another variable input, with one AND gate having an inverter on this variable input. It was therefore important to see that, when doxycycline is constantly present, blue light effectively

switched BMP-2 production on and off. Despite some background levels of BMP-2 mRNA detectable in the Doxycycline +/ Light – group, the robust activation of BMP-2 upon light stimulation allows for modulation of elements to mitigate this background to acceptable levels. One strategy to accomplish this background reduction would be to use a less powerful promoter to drive SP-dCas9-VPR production. The comparison of CMV vs EF1a promoters showed that the less powerful EF1a reduced the background, while still maintaining robust light-induced activation of BMP-2. It could also be possible to reduce the availability of SP-dCas9-VPR via plasmid ratios in transient transfections, or by integrating the vectors into the cell genome and controlling copy number. An attractive idea is to use safe harbor loci insertion (eg AAVS1). It will be important to verify that, if these strategies reduce background levels even lower, the dynamic range remains adequate, allowing for a strong upregulation of the target gene upon optogenetic stimulation.

While the concept and data presented in this chapter are a pilot study that shows an elegant solution to produce growth factor counter-gradients, further studies need to be conducted to determine the response of engineered cells to light gradients and the growth factor effects on engineered and neighboring, non-engineered, cells. Furthermore, the generation of sustained entheseal-like organization both *in vitro* and *in vivo* needs to be investigated in the future.

CHAPTER 6

CONCLUSIONS

The work presented in this dissertation was centered on three specific aims. The first was to develop an optogenetic CRISPR/Cas system to enable precise spatiotemporal control of orthogonal Cas variants. The second was to investigate the potential of delivering blue light gradients via air gap electrospun templates. Finally, the third aim was to develop a CRISPR/Cas-based, optogenetic demultiplexer circuit to enable the generation of opposing gradients of growth factors for interfacial tissue engineering, namely the enthesis. Each of these aims were explored and the data generated served as the basis for chapters 3 to 5 of this dissertation. Here we will summarize the findings of each of these chapters and then integrate the information to form cohesive, overarching conclusions regarding the work presented and how it forms a contribution to the fields of optogenetics and tissue engineering.

Chapter 3 describes the development of BluVIPR, an optogenetic system for expression of gRNAs to spatiotemporally regulate CRISPR/Cas activity. The strategy of utilizing gRNA as the output of an optogenetic RNAPII promoter is novel, and allows the BluVIPR system to be more versatile than any previous optogenetic CRISPR/Cas system described to date. We also demonstrated that BluVIPR activation of transcription is comparable to traditional Tet-On systems for chemogenetic inducibility, and exhibits lower background when compared to these. As chemogenetic inducible systems have seen widespread use and have had enormous impact in molecular biology, the comparable characteristics of an optogenetic system are auspicious, even more so when the spatiotemporal regulation inherent to optogenetics is considered. Especially important is that the dynamic range of BluVIPR activation is maintained across applications, which is a most desirable characteristic of inducible systems for synthetic biology applications.

Furthermore, we show the use of BluVIPR with two CRISPR/Cas functionalities that have never before been described to be controlled with optogenetic systems: SPnCas9-based base editors and CasRx-based CRISPR RNA interference. This showcase of the flexibility of BluVIPR is further complemented with *in vivo* experiments in zebrafish and Cas9 mice. It is especially exciting to show that BluVIPR allows the use of "off-the-shelf" transgenic Cas9 mice, as this effectively paves the way for optogenetic experiments in mouse models without the tedious and time-consuming task of generating transgenic mice tailored to each optogenetic application. The prospect of, for example, inducing precise, spatiotemporally-regulated, somatic mutations in mouse models is extremely attractive for the cancer field, among others.

In Chapter 4, we describe the investigation of blue light gradient formation on air gap electrospun templates. This first description of light forms gradients across templates that are commonly used in tissue engineering sets a framework for the inclusion of biomaterial-mediated optogenetics in regenerative medicine. The templates described in this chapter exhibited similar morphology and mechanical properties to native tendons and ligaments. These biomimetic properties should aid the formation of tendon/ligament-like tissues, and are important considerations for any tissue engineered construct. In addition, the templates presented gradients of blue light of comparable length to the depth of native entheses in the knee. Since the gradient stimulation of engineered cells is predicted to produce a gradient of growth factors, the generation of appropriately scaled light gradients is an important finding. Facile generation of light gradients that lead to growth factor gradients is an attractive solution to the problem of precise spatiotemporal presentation of signals to cells in tissue engineering. Approaches to this problem are often complex, requiring advanced manufacturing techniques and the use of expensive recombinant growth factors in supraphysiological doses, increasing cost, complexity,

and potential side effects. Integration of a suitable, perhaps even biodegradable, light source into well-established templates would present an elegant alternative strategy when precise spatiotemporal patterning of growth factors is desired.

The engineered cells referred to in chapter 4 would have to include a synthetic gene regulatory network composed of a circuit that enables the interpretation of light stimuli to generate the opposed gradients of growth factors necessary for interfacial tissue structure regeneration. In chapter 5, we described the conceptual design of a digital demultiplexer circuit based on BluVIPR activation of CRISPRa and Anti-CRISPR proteins. In this design, blue light would activate the transcription of gRNAs to target CRISPRa, effectively inducing transcription of a growth factor (as shown in chapter 3), and, concomitantly, activate the expression of an Anti-CRISPR protein targeting an orthologous Cas, effectively inhibiting the transcriptional activation of another target growth factor. This behavior is consistent with combinatorial logic attributed to a binary decoder, where the input (in this case blue light) acts as a switch to influence two different outputs in opposing fashion. We demonstrate the creation of the basic circuit component of this demultiplexer, a chemo-optogenetic AND gate, where blue light and doxycycline act as inputs to drive the activation of BMP-2. We also describe the generation of an AND gate with an inverted input (light driving Anti-CRISPR), inhibiting the activation of PDGFB. We hypothesize that such a circuit would create polarization of engineered cells towards BMP-2^{high}/PDGFB^{low} and PDGFB^{high}/BMP-2^{low} cells depending on light stimuli or lack thereof, respectively. A simple, genetically-encoded synthetic gene circuit that could drive growth factor production in a precise spatiotemporal fashion is an attractive alternative to the use of recombinant growth factors. Such a circuit would provide a cost-efficient solution to controlling cell function to precisely drive cellular behavior in a human-directed manner.

As seen above, the work described in chapters 3, 4, and 5 are interesting and provide the basis for exciting future work independently, but act together if one syncretises the findings and developments of each of these chapters into one system for interfacial tissue engineering. In such a system, one can envision air gap electrospun templates seeded with demultiplexer-engineered cells being used for ACL reconstruction, for example. The gold standard surgical technique of femoral and tibial tunnel fixation of a graft (both all-inside and outside-in techniques should be amenable) allows for convenient placement of a light source anchored in the bone, illuminating the template and generating a blue light gradient that dissipates towards the "ligament" portion of the graft. This light gradient would stimulate the engineered cells, which would generate opposed gradients of BMP-2 and PDGFB. The cells would polarize to BMP-2^{high}/$PDGFB^{low}$ at the highest light intensity, driving bone regeneration. As the light intensity subsides along the gradient, cells transition gradually towards $PDGFB^{high}$/BMP-2^{low}, creating a gradient of cell morphology and ECM remodeling reminiscent of the native enthesis. This strategy would utilize simple, cost-effective materials and require only minor modifications of the current surgical reconstruction approaches.

With a modicum of imagination, similar approaches to different research questions and therapeutic goals requiring gradients of cellular function can be envisioned. Likewise, the flexibility of the BluVIPR system lends itself to the conceptualization and generation of other synthetic genetic regulatory circuits, and combining these to form logic to suit diverse applications. Furthermore, the exploration of how to use biomaterials for optogenetic control in applications requiring spatiotemporal control could lead to more complex and varied uses. The

proposed framework for continued development of these systems will be described in the recommendations for future work section of this dissertation.

The successful development of an orthogonal optogenetic CRISPR/Cas system, BluVIPR, was the centerpiece of this dissertation, and was presented alongside the supporting evidence for biomaterial-mediated use of such a system, and the implementation of BluVIPR in a demultiplexer circuit to drive engineered cell behavior. Overall, the impact of BluVIPR revolves around the flexibility of this approach. We are excited to present this tool to the molecular biology and tissue engineering communities, and await the creative uses of it to expand the current body of knowledge.

CHAPTER 7

RECOMMENDATIONS FOR FUTURE WORK

It is an axiom that there are no finished works in science, and every new discovery leads to new questions, like the Hydra's heads. Here, we propose directions for future work in both the BluVIPR system, as well as the biomaterial-mediated optogenetic strategy.

BluVIPR

There are at least three main avenues to explore in order to improve and increase the potential impact of the BluVIPR system. First, generation of viral vectors that enable the use of the system with hard to transfect cells (e.g. primary cells) would greatly increase the feasibility of using BluVIPR in varied applications. Second, establishment of software to assist final users in the development of RGR architecture and cloning strategies into the BluVIPR constructs would increase user-friendliness and reduce barriers to entry. Third, the generation of a BluVIPR mouse would facilitate the use of this system with available mouse models, requiring only the delivery of the C120 minimal promoter and the RGR sequence.

Viral Vectors

Viral vectors would benefit greatly from reduced size for efficient packaging and increased viral titer. To this aim, we propose the development of a smaller VPR-EL222. We would approach this by first exploring the option of using a more compact VPR, and versions up to 60% of the size of conventional VPR have been described in recent literature and are available through Addgene, e.g MiniVPR. The sequence for this miniature VPR would be cloned into the BluVIPR vector and functionality would be assessed as outlined for the original system in chapter 3. After a functioning, smaller VPR-EL222 is developed, the use of cargo-limited viruses

like gamma retroviral vectors (e.g. Mouse Stem Cell Virus) would be an option. The next step would be to generate lentiviral and gamma retroviral vectors and evaluate their performance.

Software

The design of RGRs has a few complicating factors, such as the Hammer Head ribozyme complementarity requirements of downstream sequences for efficient cleavage. While a user with experience in designing and cloning relatively complex vectors would be able to successfully generate RGRs and implement the BluVIPR system, we envision a simple software that would allow other users to use BluVIPR with ease. Such a program would require the end user to design the gRNA sequence of choice with any of the available gRNA design tools. This sequence would then be input into the graphic user interface, and variables such as species of Cas and version of BluVIPR vector would be chosen. With this information, the program would generate a sequence including appropriate type IIs restriction enzyme recognition sequences (creating overhangs compatible with the BluVIPR vector specified) and a fully functional RGR with the appropriate gRNA scaffold for the specified Cas.

BluVIPR Mouse

While cells from available Cas mice can be modified *ex vivo* with the viral vectors described earlier, applications that require delivery without cells being removed from the host would greatly benefit from the availability of a BluVIPR mouse. In such a strategy, VPR-EL222 would be integrated into a safe harbor locus (e.g. ROSA26). An efficient way of generating knock-in mice with CRISPR/Cas9 has been described by Chu et al. (Rajewsky group) and would be a viable option. In summary, Cas9 and gRNA RNPs are injected into blastocysts. This gRNA targets the intronic XbaI site of ROSA26 and, when an appropriate template DNA is provided, allows for homology directed repair to induce knock-ins in up to 50% of injected embryos. Once

transgenic mice expressing VPR-EL222 are generated, these could be crossed with available Cas mice to create transgenic mice that express both Cas9 and VPR-EL222. This would allow the generation of very small (around 1kb) cargo containing C120 and RGR sequences, packagable in even AAV vectors.

BIOMATERIAL-MEDIATED OPTOGENETICS

To expand on the proof of concept for biomaterials as optogenetic tools presented in this dissertation, we propose the exploration of light gradient modulation by material properties, and the investigation into other fabrication strategies and how their products interact with light. To characterize how material properties modulate light gradients, fabrication of electrospun templates of different biomaterials and with varying porosity, fiber morphology, and combinations of these, followed by light gradient analysis as outlined in chapter 4 would lead to finding conditions that affect the generation of light gradients. Using these parameters in design of templates for biomaterial-mediated optogenetics would allow for precise control of the desired presentation of spatiotemporal stimuli. On the other hand, exploring how other fabrication techniques aside from electrospinning, like additive manufacturing or hydrogel production, generate templates with different optical qualities would expand the use of optogenetic tools with biomaterials. To this end, templates generated with different fabrication techniques would be evaluated as outlined in chapter 4 and compared to each other to create a database of desired material properties coupled with optical properties.

REFERENCES

1. Yamada, M., Nagasaki, S. C., Ozawa, T. & Imayoshi, I. Light-mediated control of Gene expression in mammalian cells. *Neuroscience Research* **152**, 66–77 (2020).
2. Polstein, L. R. & Gersbach, C. A. Light-Inducible Spatiotemporal Control of Gene Activation by Customizable Zinc Finger Transcription Factors. *J Am Chem Soc* **134**, 16480–16483 (2012).
3. Polstein, L. R. & Gersbach, C. A. A light-inducible CRISPR/Cas9 system for control of endogenous gene activation. *Nat Chem Biol* **11**, 198–200 (2015).
4. Shimizu-Sato, S., Huq, E., Tepperman, J. M. & Quail, P. H. A light-switchable gene promoter system. *Nat. Biotechnol.* **20**, 1041–1044 (2002).
5. Lu, J. *et al.* Multimode drug inducible CRISPR/Cas9 devices for transcriptional activation and genome editing. *Nucleic Acids Res.* **46**, e25 (2018).
6. Gangopadhyay, S. A. *et al.* Precision Control of CRISPR-Cas9 Using Small Molecules and Light. *Biochemistry* **58**, 234–244 (2019).
7. Zhou, X. X. *et al.* A Single-Chain Photoswitchable CRISPR-Cas9 Architecture for Light-Inducible Gene Editing and Transcription. *ACS Chem. Biol.* **13**, 443–448 (2018).
8. Jain, P. K. *et al.* Development of Light-Activated CRISPR Using Guide RNAs with Photocleavable Protectors. *Angewandte Chemie International Edition* **55**, 12440–12444 (2016).
9. Liu, Y. *et al.* Very fast CRISPR on demand. *Science* **368**, 1265–1269 (2020).
10. Skår, J. *et al.* Self–organized living systems: conjunction of a stable organization with chaotic fluctuations in biological space–time. *Philosophical Transactions of the Royal*

Society of London. Series A: Mathematical, Physical and Engineering Sciences **361**, 1125–1139 (2003).

11. Gare, A. Chreods, homeorhesis and biofields: Finding the right path for science through Daoism. *Progress in Biophysics and Molecular Biology* **131**, 61–91 (2017).
12. Fuente, I. M. D. la *et al.* On the Dynamics of the Adenylate Energy System: Homeorhesis vs Homeostasis. *PLOS ONE* **9**, e108676 (2014).
13. Mamontov, E. Modelling homeorhesis by ordinary differential equations. *Mathematical and Computer Modelling* **45**, 694–707 (2007).
14. Matsushita, Y. & Kaneko, K. Homeorhesis in Waddington's landscape by epigenetic feedback regulation. *Phys. Rev. Research* **2**, 023083 (2020).
15. Wiener, N. *Cybernetics or Control and Communication in the Animal and the Machine, Reissue of the 1961 second edition*. (MIT Press, 2019).
16. Amen, R. D. A Biological Systems Concept. *BioScience* **16**, 396–401 (1966).
17. Wolkenhauer, O. Systems biology: The reincarnation of systems theory applied in biology? *Brief Bioinform* **2**, 258–270 (2001).
18. Giuseppin, M. L. F. & van Riel, N. A. W. Metabolic Modeling of Saccharomyces cerevisiae Using the Optimal Control of Homeostasis: A Cybernetic Model Definition. *Metabolic Engineering* **2**, 14–33 (2000).
19. Wallach, D. The cybernetics of TNF: Old views and newer ones. *Seminars in Cell & Developmental Biology* **50**, 105–114 (2016).
20. Hashimshony, T., Feder, M., Levin, M., Hall, B. K. & Yanai, I. Spatiotemporal transcriptomics reveals the evolutionary history of the endoderm germ layer. *Nature* **519**, 219–222 (2015).

21. Morckel, A. R. *et al.* A photoactivatable small-molecule inhibitor for light-controlled spatiotemporal regulation of Rho kinase in live embryos. *Development* **139**, 437–442 (2012).

22. Meyer, T. N. *et al.* Spatiotemporal regulation of morphogenetic molecules during in vitro branching of the isolated ureteric bud: toward a model of branching through budding in the developing kidney. *Developmental Biology* **275**, 44–67 (2004).

23. Atwood, C. S. & Vadakkadath Meethal, S. The spatiotemporal hormonal orchestration of human folliculogenesis, early embryogenesis and blastocyst implantation. *Molecular and Cellular Endocrinology* **430**, 33–48 (2016).

24. Sandhu, K. S., Li, G., Sung, W.-K. & Ruan, Y. Chromatin interaction networks and higher order architectures of eukaryotic genomes. *Journal of Cellular Biochemistry* **112**, 2218–2221 (2011).

25. Kim, M.-S., Kim, J.-R., Kim, D., Lander, A. D. & Cho, K.-H. Spatiotemporal network motif reveals the biological traits of developmental gene regulatory networks in Drosophila melanogaster. *BMC Syst Biol* **6**, 31 (2012).

26. Wan, G. *et al.* Spatiotemporal regulation of liquid-like condensates in epigenetic inheritance. *Nature* **557**, 679–683 (2018).

27. Zhang, S., Charest, P. G. & Firtel, R. A. Spatiotemporal Regulation of Ras Activity Provides Directional Sensing. *Current Biology* **18**, 1587–1593 (2008).

28. Gerstenfeld, L. C., Cullinane, D. M., Barnes, G. L., Graves, D. T. & Einhorn, T. A. Fracture healing as a post-natal developmental process: Molecular, spatial, and temporal aspects of its regulation. *Journal of Cellular Biochemistry* **88**, 873–884 (2003).

29. Schibler, U. The daily rhythms of genes, cells and organs. *EMBO reports* **6**, S9–S13 (2005).

30. Schwartz, W. J. & Meijer, J. H. Real-time imaging reveals spatiotemporal dynamics of cellular circadian clocks. *Trends in Neurosciences* **27**, 513–516 (2004).

31. Evans, J. A., Leise, T. L., Castanon-Cervantes, O. & Davidson, A. J. Intrinsic Regulation of Spatiotemporal Organization within the Suprachiasmatic Nucleus. *PLOS ONE* **6**, e15869 (2011).

32. Paganelli, R., Petrarca, C. & Di Gioacchino, M. Biological clocks: their relevance to immune-allergic diseases. *Clinical and Molecular Allergy* **16**, 1 (2018).

33. Hogenesch, J. B., Panda, S., Kay, S. & Takahashi, J. S. Circadian Transcriptional Output in the SCN and Liver of the Mouse. in *Molecular Clocks and Light Signalling* 171–183 (John Wiley & Sons, Ltd, 2008). doi:10.1002/0470090839.ch13.

34. Balling, R. From mouse genetics to systems biology. *Mamm Genome* **18**, 383–388 (2007).

35. Saez, E., No, D., West, A. & Evans, R. M. Inducible gene expression in mammalian cells and transgenic mice. *Current Opinion in Biotechnology* **8**, 608–616 (1997).

36. Clackson, T. Controlling mammalian gene expression with small molecules. *Current Opinion in Chemical Biology* **1**, 210–218 (1997).

37. Fussenegger, M. *et al.* Streptogramin-based gene regulation systems for mammalian cells. *Nature Biotechnology* **18**, 1203–1208 (2000).

38. Gupta, S., Schoer, R. A., Egan, J. E., Hannon, G. J. & Mittal, V. Inducible, reversible, and stable RNA interference in mammalian cells. *PNAS* **101**, 1927–1932 (2004).

39. Kappel, S., Matthess, Y., Kaufmann, M. & Strebhardt, K. Silencing of mammalian genes by tetracycline-inducible shRNA expression. *Nature Protocols* **2**, 3257–3269 (2007).

40. Wu, R.-H. *et al.* A tightly regulated and reversibly inducible siRNA expression system for conditional RNAi-mediated gene silencing in mammalian cells. *The Journal of Gene Medicine* **9**, 620–634 (2007).

41. Gossen, M. & Bujard, H. Tight control of gene expression in mammalian cells by tetracycline-responsive promoters. *PNAS* **89**, 5547–5551 (1992).

42. No, D., Yao, T. P. & Evans, R. M. Ecdysone-inducible gene expression in mammalian cells and transgenic mice. *PNAS* **93**, 3346–3351 (1996).

43. Madio, D. P. *et al.* Invited. On the feasibility of MRI-guided focused ultrasound for local induction of gene expression. *Journal of Magnetic Resonance Imaging* **8**, 101–104 (1998).

44. Gerner, E. W. *et al.* Heat-inducible vectors for use in gene therapy. *International Journal of Hyperthermia* **16**, 171–181 (2000).

45. Yang, W. & Paschen, W. Conditional gene silencing in mammalian cells mediated by a stress-inducible promoter. *Biochemical and Biophysical Research Communications* **365**, 521–527 (2008).

46. McCarrey, J. R. Evolution of Tissue-Specific Gene Expression in Mammals. *BioScience* **44**, 20–27 (1994).

47. Miyoshi, G. & Fishell, G. Directing neuron-specific transgene expression in the mouse CNS. *Current Opinion in Neurobiology* **16**, 577–584 (2006).

48. Kos, C. H. Methods in Nutrition Science: Cre/loxP System for Generating Tissue-specific Knockout Mouse Models. *Nutr Rev* **62**, 243–246 (2004).

49. Gutierrez, A. A., Lemoine, N. R. & Sikora, K. Gene therapy for cancer. *The Lancet* **339**, 715–721 (1992).

50. Smith, A. D., Sumazin, P. & Zhang, M. Q. Tissue-specific regulatory elements in mammalian promoters. *Molecular Systems Biology* **3**, 73 (2007).

51. Tiyaboonchai, A. *et al.* Utilization of the AAVS1 safe harbor locus for hematopoietic specific transgene expression and gene knockdown in human ES cells. *Stem Cell Research* **12**, 630–637 (2014).

52. Liu, B. H., Wang, X., Ma, Y. X. & Wang, S. CMV enhancer/human PDGF-β promoter for neuron-specific transgene expression. *Gene Therapy* **11**, 52–60 (2004).

53. Morton, S. K., Chaston, D. J., Baillie, B. K., Hill, C. E. & Matthaei, K. I. Regulation of Endothelial-Specific Transgene Expression by the LacI Repressor Protein In Vivo. *PLOS ONE* **9**, e95980 (2014).

54. Fishman Glenn I. Timing Is Everything in Life. *Circulation Research* **82**, 837–844 (1998).

55. Liu, B., Wang, S., Brenner, M., Paton, J. F. R. & Kasparov, S. Enhancement of cell-specific transgene expression from a Tet-Off regulatory system using a transcriptional amplification strategy in the rat brain. *The Journal of Gene Medicine* **10**, 583–592 (2008).

56. Osterwalder, T., Yoon, K. S., White, B. H. & Keshishian, H. A conditional tissue-specific transgene expression system using inducible GAL4. *PNAS* **98**, 12596–12601 (2001).

57. Bacaj, T. & Shaham, S. Temporal Control of Cell-Specific Transgene Expression in Caenorhabditis elegans. *Genetics* **176**, 2651–2655 (2007).

58. Sauer, B. Functional expression of the cre-lox site-specific recombination system in the yeast Saccharomyces cerevisiae. *Molecular and Cellular Biology* **7**, 2087–2096 (1987).

59. Ristevski, S. Making better transgenic models. *Mol Biotechnol* **29**, 153–163 (2005).

60. Ausländer, D. *et al.* A Synthetic Multifunctional Mammalian pH Sensor and CO2 Transgene-Control Device. *Molecular Cell* **55**, 397–408 (2014).

61. Doudna, J. A. & Mali, P. *CRISPR-Cas: a laboratory manual*. (Cold Spring Harbor Laboratory Press, 2016).

62. Mali, P. *et al.* RNA-Guided Human Genome Engineering via Cas9. *Science* **339**, 823–826 (2013).

63. Perez-Pinera, P. *et al.* RNA-guided gene activation by CRISPR-Cas9-based transcription factors. *Nat Meth* **10**, 973–976 (2013).

64. Larson, M. H. *et al.* CRISPR interference (CRISPRi) for sequence-specific control of gene expression. *Nature Protocols* **8**, 2180–2196 (2013).

65. Gilbert, L. A. CRISPR-mediated modular RNA-guided regulation of transcription in eukaryotes. *Cell* **154**, 442–451 (2013).

66. Rees, H. A. & Liu, D. R. Base editing: precision chemistry on the genome and transcriptome of living cells. *Nature Reviews Genetics* **19**, 770–788 (2018).

67. Hess, G. T., Tycko, J., Yao, D. & Bassik, M. C. Methods and Applications of CRISPR-Mediated Base Editing in Eukaryotic Genomes. *Molecular Cell* **68**, 26–43 (2017).

68. Chavez, A. *et al.* Highly efficient Cas9-mediated transcriptional programming. *Nat. Methods* **12**, 326–328 (2015).

69. Makarova, K. S., Wolf, Y. I. & Koonin, E. V. Classification and Nomenclature of CRISPR-Cas Systems: Where from Here? *The CRISPR Journal* **1**, 325–336 (2018).

70. Makarova, K. S. *et al.* Evolution and classification of the CRISPR–Cas systems. *Nature Reviews Microbiology* **9**, 467–477 (2011).

71. Koonin, E. V., Makarova, K. S. & Zhang, F. Diversity, classification and evolution of CRISPR-Cas systems. *Current Opinion in Microbiology* **37**, 67–78 (2017).

72. Zetsche, B. *et al.* Cpf1 Is a Single RNA-Guided Endonuclease of a Class 2 CRISPR-Cas System. *Cell* **163**, 759–771 (2015).

73. Alok, A. *et al.* The Rise of the CRISPR/Cpf1 System for Efficient Genome Editing in Plants. *Front. Plant Sci.* **11**, (2020).

74. Konermann, S. *et al.* Transcriptome Engineering with RNA-Targeting Type VI-D CRISPR Effectors. *Cell* **173**, 665-676.e14 (2018).

75. Fenno, L., Yizhar, O. & Deisseroth, K. The Development and Application of Optogenetics. *Annual Review of Neuroscience* **34**, 389–412 (2011).

76. Guru, A., Post, R. J., Ho, Y.-Y. & Warden, M. R. Making Sense of Optogenetics. *Int J Neuropsychopharmacol* **18**, (2015).

77. Boyden, E. S., Zhang, F., Bamberg, E., Nagel, G. & Deisseroth, K. Millisecond-timescale, genetically targeted optical control of neural activity. *Nature Neuroscience* **8**, 1263–1268 (2005).

78. Pathak, G. P., Vrana, J. D. & Tucker, C. L. Optogenetic control of cell function using engineered photoreceptors. *Biology of the Cell* **105**, 59–72 (2013).

79. Deisseroth, K. Optogenetics and Psychiatry: Applications, Challenges, and Opportunities. *Biological Psychiatry* **71**, 1030–1032 (2012).

80. Biselli, T., Lange, S. S., Sablottny, L., Steffen, J. & Walther, A. Optogenetic and chemogenetic insights into the neurocircuitry of depression-like behaviour: A systematic review. *European Journal of Neuroscience* **n/a**,.

81. Bentley, J. N., Chestek, C., Stacey, W. C. & Patil, P. G. Optogenetics in epilepsy. *Neurosurgical Focus* **34**, E4 (2013).

82. Carter, M. E. & de Lecea, L. Optogenetic investigation of neural circuits in vivo. *Trends in Molecular Medicine* **17**, 197–206 (2011).

83. Montgomery, K. L., Iyer, S. M., Christensen, A. J., Deisseroth, K. & Delp, S. L. Beyond the brain: Optogenetic control in the spinal cord and peripheral nervous system. *Science Translational Medicine* **8**, 337rv5-337rv5 (2016).

84. Grosenick, L., Marshel, J. H. & Deisseroth, K. Closed-Loop and Activity-Guided Optogenetic Control. *Neuron* **86**, 106–139 (2015).

85. Entcheva, E. Cardiac optogenetics. *American Journal of Physiology-Heart and Circulatory Physiology* **304**, H1179–H1191 (2013).

86. Johnson, H. E. & Toettcher, J. E. Illuminating developmental biology with cellular optogenetics. *Current Opinion in Biotechnology* **52**, 42–48 (2018).

87. Pudasaini, A., El-Arab, K. K. & Zoltowski, B. D. LOV-based optogenetic devices: light-driven modules to impart photoregulated control of cellular signaling. *Front. Mol. Biosci.* **2**, (2015).

88. Zhang, K. & Cui, B. Optogenetic control of intracellular signaling pathways. *Trends in Biotechnology* **33**, 92–100 (2015).

89. Rivera-Cancel, G., Motta-Mena, L. B. & Gardner, K. H. Identification of natural and artificial DNA substrates for the light-activated LOV-HTH transcription factor EL222. *Biochemistry* **51**, 10024–10034 (2012).

90. Motta-Mena, L. B. *et al.* An optogenetic gene expression system with rapid activation and deactivation kinetics. *Nature Chemical Biology* **10**, 196–202 (2014).

91. Reade, A. *et al.* TAEL: a zebrafish-optimized optogenetic gene expression system with fine spatial and temporal control. *Development* **144**, 345–355 (2017).

92. Ausländer, D. & Fussenegger, M. Optogenetic Therapeutic Cell Implants. *Gastroenterology* **143**, 301–306 (2012).

93. Font Tellado, S., Balmayor, E. R. & Van Griensven, M. Strategies to engineer tendon/ligament-to-bone interface: Biomaterials, cells and growth factors. *Advanced Drug Delivery Reviews* **94**, 126–140 (2015).

94. Apostolakos, J. *et al.* The enthesis: a review of the tendon-to-bone insertion. *Muscles Ligaments Tendons J* **4**, 333–342 (2014).

95. Lu, H. H. & Thomopoulos, S. Functional attachment of soft tissues to bone: development, healing, and tissue engineering. *Annu Rev Biomed Eng* **15**, 201–226 (2013).

96. Benjamin, M. & Ralphs, J. R. Entheses--the bony attachments of tendons and ligaments. *Ital J Anat Embryol* **106**, 151–157 (2001).

97. Min, H. K., Oh, S. H., Lee, J. M., Im, G. I. & Lee, J. H. Porous membrane with reverse gradients of PDGF-BB and BMP-2 for tendon-to-bone repair: in vitro evaluation on adipose-derived stem cell differentiation. *Acta Biomater* **10**, 1272–1279 (2014).

98. Hankenson, K. D., Gagne, K. & Shaughnessy, M. Extracellular signaling molecules to promote fracture healing and bone regeneration. *Adv. Drug Deliv. Rev.* **94**, 3–12 (2015).

99. Hee, C. K., Dines, J. S., Solchaga, L. A., Shah, V. R. & Hollinger, J. O. Regenerative tendon and ligament healing: opportunities with recombinant human platelet-derived growth factor BB-homodimer. *Tissue Eng Part B Rev* **18**, 225–234 (2012).

100. Zhang, Y., Cheng, N., Miron, R., Shi, B. & Cheng, X. Delivery of PDGF-B and BMP-7 by mesoporous bioglass/silk fibrin scaffolds for the repair of osteoporotic defects. *Biomaterials* **33**, 6698–6708 (2012).

101. Babensee, J. E., McIntire, L. V. & Mikos, A. G. Growth Factor Delivery for Tissue Engineering. *Pharm Res* **17**, 497–504 (2000).

102. Cong, L. *et al.* Multiplex genome engineering using CRISPR/Cas systems. *Science* **339**, 819–823 (2013).

103. Jinek, M. *et al.* A Programmable Dual-RNA–Guided DNA Endonuclease in Adaptive Bacterial Immunity. *Science* **337**, 816–821 (2012).

104. Alford, S. C., Wu, J., Zhao, Y., Campbell, R. E. & Knöpfel, T. Optogenetic reporters. *Biology of the Cell* **105**, 14–29 (2013).

105. Gao, Y. & Zhao, Y. Self-processing of ribozyme-flanked RNAs into guide RNAs in vitro and in vivo for CRISPR-mediated genome editing. *Journal of Integrative Plant Biology* **56**, 343–349 (2014).

106. Sakata, R. C. *et al.* Base editors for simultaneous introduction of C-to-T and A-to-G mutations. *Nat. Biotechnol.* **38**, 865–869 (2020).

107. Grünewald, J. *et al.* CRISPR DNA base editors with reduced RNA off-target and self-editing activities. *Nat. Biotechnol.* **37**, 1041–1048 (2019).

108. Covacu, R., Perez Estrada, C., Arvidsson, L., Svensson, M. & Brundin, L. Change of fate commitment in adult neural progenitor cells subjected to chronic inflammation. *J. Neurosci.* **34**, 11571–11582 (2014).

109. Johansson, C. B. *et al.* Identification of a neural stem cell in the adult mammalian central nervous system. *Cell* **96**, 25–34 (1999).

110. Garg, K. & Bowlin, G. L. Electrospinning jets and nanofibrous structures. *Biomicrofluidics* **5**, 013403 (2011).

111. Sell, S. A., McClure, M. J., Ayres, C. E., Simpson, D. G. & Bowlin, G. L. Preliminary Investigation of Airgap Electrospun Silk-Fibroin-Based Structures for Ligament Analogue Engineering. *Journal of Biomaterials Science, Polymer Edition* **22**, 1253–1273 (2011).

112. Jha, B. S. *et al.* Two pole air gap electrospinning: Fabrication of highly aligned, three-dimensional scaffolds for nerve reconstruction. *Acta Biomaterialia* **7**, 203–215 (2011).

113. Zhao, L., Thambyah, A. & Broom, N. D. A multi-scale structural study of the porcine anterior cruciate ligament tibial enthesis. *Journal of Anatomy* **224**, 624–633 (2014).

114. Pal, S. *Design of Artificial Human Joints & Organs*. (Springer US, 2014). doi:10.1007/978-1-4614-6255-2.

115. Butler, D. L. *et al.* Location-dependent variations in the material properties of the anterior cruciate ligament. *J Biomech* **25**, 511–518 (1992).

116. Dimitriou, R. *et al.* Application of recombinant BMP-7 on persistent upper and lower limb non-unions. *Injury* **36**, S51–S59 (2005).

117. Haidar, Z. S., Hamdy, R. C. & Tabrizian, M. Delivery of recombinant bone morphogenetic proteins for bone regeneration and repair. Part A: Current challenges in BMP delivery. *Biotechnol Lett* **31**, 1817 (2009).

118. Epstein, N. E. Complications due to the use of BMP/INFUSE in spine surgery: The evidence continues to mount. *Surg Neurol Int* **4**, S343–S352 (2013).

119. Borges, A. L., Davidson, A. R. & Bondy-Denomy, J. The Discovery, Mechanisms, and Evolutionary Impact of Anti-CRISPRs. *Annu Rev Virol* **4**, 37–59 (2017).

120. Stanley, S. Y. & Maxwell, K. L. Phage-Encoded Anti-CRISPR Defenses. *Annu. Rev. Genet.* **52**, 445–464 (2018).

121. Marino, N. D., Pinilla-Redondo, R., Csörgő, B. & Bondy-Denomy, J. Anti-CRISPR protein applications: natural brakes for CRISPR-Cas technologies. *Nature Methods* **17**, 471–479 (2020).

122. Maini, A. K. *Digital Electronics: Principles, Devices and Applications*. (Wiley, 2007).